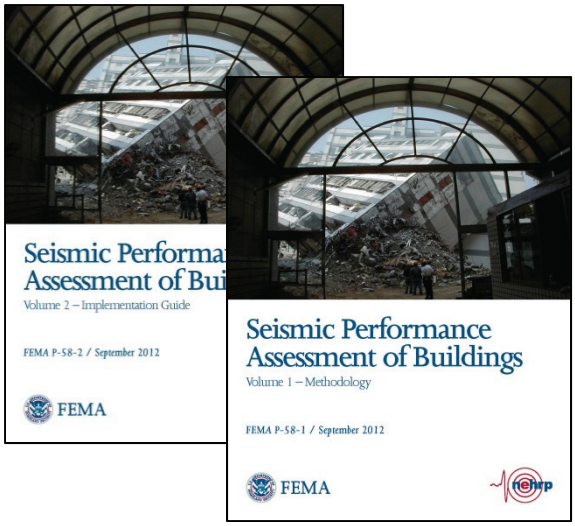

Background Document

FEMA P-58/BD-3.7.16

PACT Beta Test Example: Building C Reinforced Masonry Shear Wall Building

Prepared by

Benson Shing and Juan Murcia-Delso
Department of Structural Engineering
University of California, San Diego
La Jolla, California 92093

Submitted to

APPLIED TECHNOLOGY COUNCIL
201 Redwood Shores Parkway, Suite 240
Redwood City, California 94065
www.ATCouncil.org

Prepared for

FEDERAL EMERGENCY MANAGEMENT AGENCY
U.S. Department of Homeland Security
500 C Street, SW
Washington, D.C. 20472

March 14, 2013

FEMA

nehrp

Background Documentation

FEMA P-58 Background Documents are a series of reports documenting the technical background and source information for key aspects of the FEMA P-58 methodology and its implementation. These reports were developed over the course of the 10-year ATC-58/ATC-58-1 Projects funded under FEMA Contracts EMW-2001-RP-0056 and HSFEHQ-06-D-1105.

Background Documents were developed by consultants, serving at various levels within the project hierarchy, reporting the results of: (1) decisions on technical development protocols; (2) focused studies on the development of key aspects of the methodology; (3) documentation of recommended procedures; and (4) collection of available data for the development of structural and nonstructural fragilities. They were initially intended to serve as a record of the technical state-of-knowledge at the time they were produced, and as resources for the development of the eventual project reports. As such, they represent a snapshot in time, and may, or may not, match the technical content, recommended procedures, or data incorporated into the final methodology and its implementation.

This Background Document is intended for the purpose of providing supplemental knowledge to users of the FEMA P-58 methodology. Information contained herein has not been independently verified for accuracy as a stand-alone document, and may have been superseded in its final implementation within the methodology. Users of information in this document assume all liability arising from such use.

Notice

Cover illustration – Primary resource documents for the FEMA P-58 *Seismic Performance Assessment of Buildings, Methodology and Implementation* series of products: FEMA P-58-1, *Volume 1 – Methodology*, and FEMA P-58-2, *Volume 2 – Implementation Guide*.

PACT Beta Test Example: Building C Reinforced Masonry Shear Wall Building

Prepared by

Benson Shing
Juan Murcia-Delso
University of California, San Diego

March 14, 2013

1.1 Reinforced Masonry Shear Wall Building Example

1.1.1 Introduction and Overview

This section presents the seismic performance assessment of a two-story building that has special load bearing reinforced masonry shear walls (RMSWs) designed according to the seismic provisions of ASCE/SEI 7-05 (ASCE/SEI 2005) and the strength design requirements of the MSJC code (MSJC 2008).

1.1.2 Description of Building and Site

Site Location and Site Hazard

The building is a hotel located at a site in Los Angeles, California, Site Class C, and is classified as Seismic Design Category (SDC) D_{max} (ATC 2009). The fundamental period of the building calculated with eigenvalue analysis is 0.13 sec. in both directions. The site location and the corresponding seismic hazard curve for the building is shown in Figure 1-1. More information about the site and seismic hazard is provided in the PACT Beta Test Overview Report, BD-3.7.13.

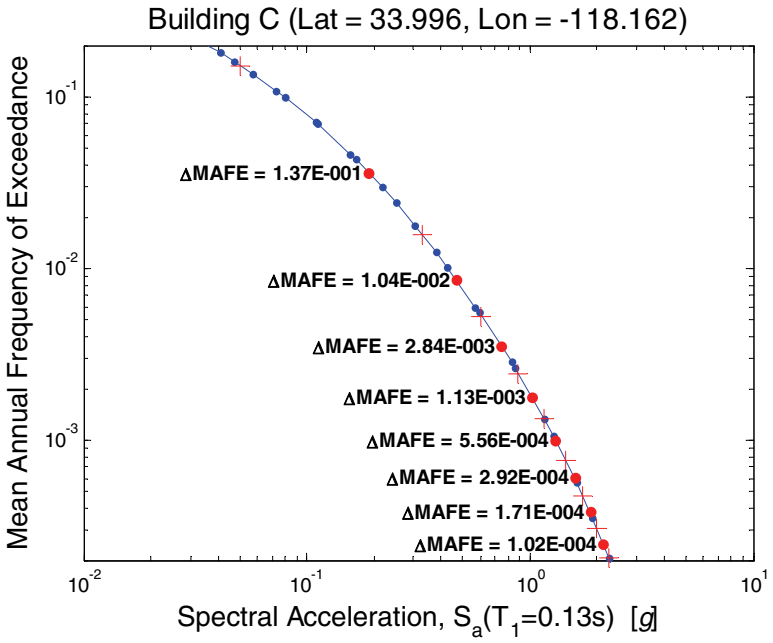

Figure 1-1 Hazard curve

Structural and Non-Structural Design

The plan and elevation views of the building are shown in Figure 1-2. The lateral force-resisting system consists of four special RMSW's in each direction. The walls are designed and detailed according to the strength design requirements of the MSJC code (MSJC 2008). The NS and EW walls have different designs because they are subjected to different gravity loads. The NS walls carry higher axial loads because they support the precast hollow-core planks, which span along the EW direction. The EW walls carry only the self-weight and loads from the hallways. All the RMSW's are fully-grouted with a story-height of 10 ft. and a plan length of 32 ft. They are constructed of concrete masonry blocks that have a nominal width of 8 in. The quantities of the vertical reinforcement in the NS and EW walls are shown in Figure 1-3. Diagonal shear failure is prohibited by following the capacity design approach stipulated in the MSJC code for special walls.

The gravity system consists of 14-in.-x-25-in. RC beams and 16-in.–x-16-in. RC columns as indicated in Figure 1-2. The quantities of non-structural components have been determined based on the building plan and the normative quantities recommended in the ATC-58 Guidelines (ATC 2011). These include exterior walls, windows, roof tiling, partitions, ceilings, an elevator, stairs, piping, HVAC system, electrical equipment, and entertainment equipment.

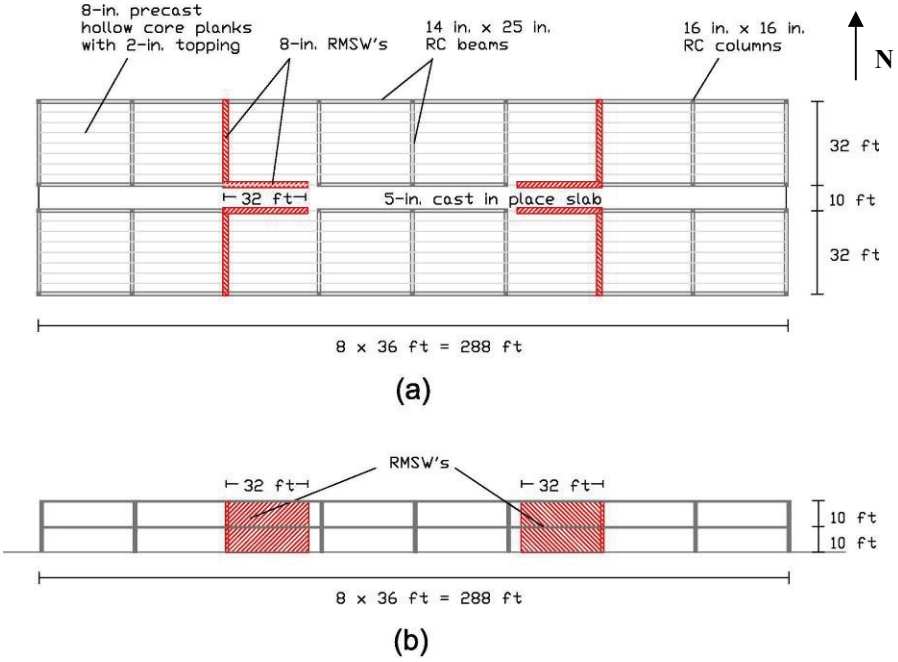

Figure 1-2 Two-story building; (a) plan view; (b) elevation view

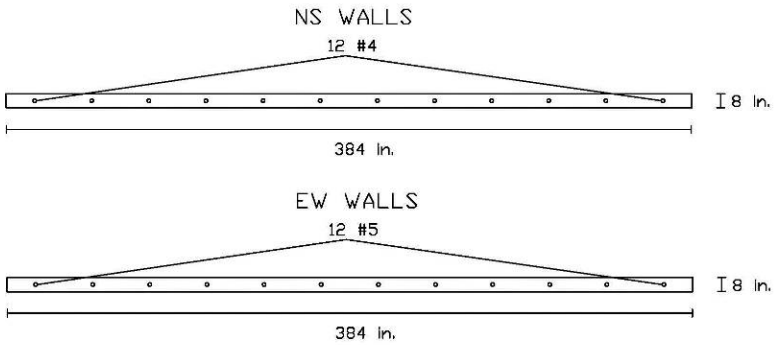

Figure 1-3 Cross-sections of NS and EW walls

1.1.3 Analysis Methods

Two types of analysis methods are permitted in the ATC-58 Guidelines (ATC 2011) for the seismic performance assessment of buildings. One is the nonlinear time-history analysis and the other is the simplified analysis based on the procedure given in the guidelines.

Nonlinear analysis. For nonlinear time-history analysis, the modeling method used here is the same as that used by Koutromanos and Shing (2010) for the ATC-76 study. In each direction, the system is idealized as an uncoupled cantilever wall with appropriate tributary gravity load and seismic mass. Since the walls in the two orthogonal directions are not structurally connected, each wall has a rectangular section. The coupling forces introduced by the roof and floor diaphragms have been ignored in the model. The base of the wall has been considered to be perfectly fixed. The analyses have been conducted with the software platform OpenSees developed by the Pacific Earthquake Engineering Research Center (PEER) using displacement-based fiber-section beam-column elements to model the flexural behavior. Shear deformation has been modeled with zero-length springs. Only one modification has been introduced with respect to the model of Koutromanos and Shing (2010). Instead of using elastic springs to model shear deformation, the bilinear law shown in Figure 1-4 has been used here to account for the decrease of shear stiffness before the peak shear capacity has been reached. The bilinear law is based on the secant shear stiffness of reinforced masonry walls measured in the tests of Shing et al. (1991). For an axial compressive stress comparable to that experienced by the walls considered in this study, the average secant shear stiffness measured was close to 20% of the theoretical elastic shear stiffness of the walls when they were loaded to the first occurrence of a major diagonal crack. Based on available test data, Murcia-Delso and Shing (2009) have found that there is a 50% chance that a major diagonal crack will develop when the base shear in

a wall reaches 86% of the nominal shear strength calculated according to the MSJC code. The wall model is shown in Figure 1-5. A more detailed explanation about the model can be found in Koutromanos and Shing (2010).

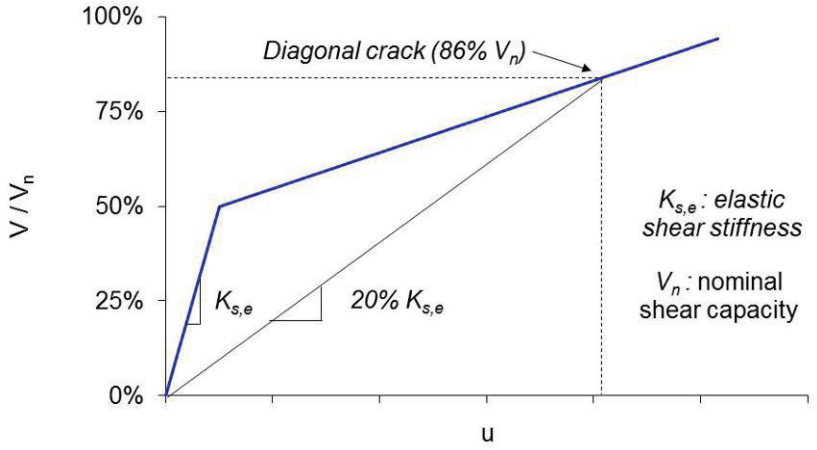

Figure 1-4 Bilinear law for shear springs

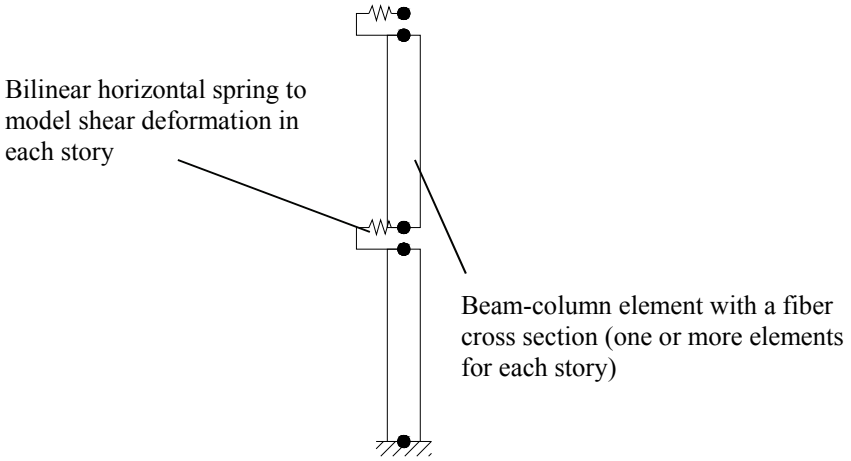

Figure 1-5 Wall model

Simplified analysis. For the simplified analysis, the procedure suggested in Section 1.3 of Volume 1 of the 90% draft of the ATC-58 Guidelines (ATC 2011) is to be followed. For this purpose, the building is again idealized as having a system of uncoupled cantilever walls. Hence, only one wall with appropriate tributary gravity load and seismic mass needs to be considered for a static lateral load analysis.

For a given earthquake intensity level, the equivalent static lateral load is determined based on the spectral acceleration corresponding to the fundamental period of the building, the soil class, the modal characteristics,

and the yield strength of the wall. The yield strength is to be taken as the maximum base shear developed in a static pushover analysis using the same nonlinear model used in the time-history analysis.

The static lateral force is distributed along the height of the building and applied at the floor and roof levels, and an elastic analysis is carried out. In the elastic analysis, the effective moment of inertia (considering possible cracking) of the wall cross section is assumed to be one-half of that of an uncracked section. The story drifts from the elastic analysis are then corrected with factors whose values depend on the geometry, the modal characteristics, and the yield strength of the wall, as given in the ATC-58 Guidelines, to account for the inelastic behavior. The floor accelerations are obtained by multiplying the peak ground acceleration with factors that depend on the same parameters mentioned above.

1.1.4 PACT Input

Building information that is needed by PACT for the seismic performance assessment is presented and explained in this section. These data are entered through different information tabs in the program as presented below.

Project Information Tab

General information for the project is input through the Project Info tab as shown in Figure 1-6 .

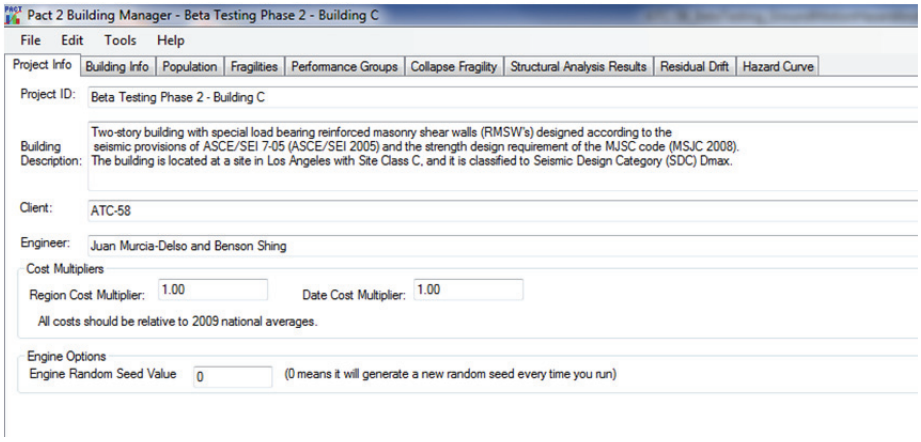

Figure 1-6 Project information tab

Building Information Tab

General information for the building is input through the Building Info tab as shown in Figure 1-7.

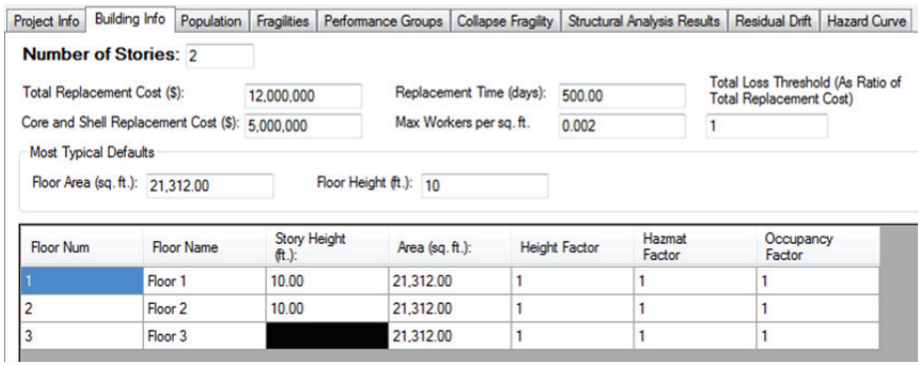

Figure 1-7 Building information tab

It is important to make a good estimation of the replacement cost for the building, which is considered as the total economic loss in the case of collapse. In this case, the replacement cost for the entire building is based on $300 per square foot of floor area. The replacement time is assumed to be 500 days.

Population Tab

The building population model defines the number of occupants per 1,000 sq. ft. of floor area at different times of the day and on different days of the year. Since this building is a hotel, a default population model for hospitality buildings in PACT has been chosen. However, the peak number of occupants per 1,000 sq. ft. has been increased from a default value of 2.5 to 4, which is perceived to be more reasonable. The population distribution on a weekday is shown in Figure 1-8 .

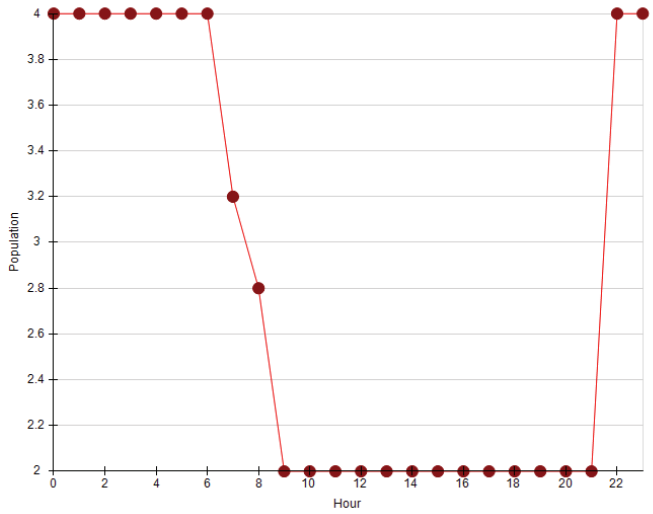

Figure 1-8 Population model for the building on a weekday (number of occupants per 1,000 sq. ft.)

Fragility Tab

Structural elements

The following fragility groups have been considered for the structural systems.

- The gravity frame system is considered ordinary moment frames, which according to PACT are quantified by a collection of beam-to-column joints. For performance assessment, the joint assemblies are distinguished according to their location in either the first or second level in the building and their orientation in direction 1 or 2. The following two fragility groups for beam-to-column joint assemblies, which best fit the system considered here, are selected from PACT for the probabilistic damage assessment.
    - *B1041.061a: ACI 318 OMF with weak columns, Conc Col & Bm = 24" x 24", Beam one side.*
    - *B1041.061b: ACI 318 OMF with weak columns, Conc Col & Bm = 24" x 24", Beam both sides*

One represents an exterior joint assembly with beam on one side only, and the other an interior joint assembly with beams on both sides. In PACT, these fragility groups are included in the first and second levels of the building and applied to directions 1 and 2.

- The RMSW's belong to one fragility group identified by PACT as B1052.004: Special reinforced masonry walls with fully grouted cells, 8" to 12" thick, flexure dominated greater than 12' tall

For this fragility group, PACT assumes that the flexural, diagonal shear, and sliding shear damage modes are mutually exclusive. The walls considered here are assumed to be flexure critical even though their failure behavior could be dominated by sliding shear because of the low aspect ratio. This assumption is based on the fact that there is a lack of reliable analytical means to model the sliding shear behavior of a wall and that there is no fragility data to relate the amount of base sliding to the level of damage. It should also be pointed out that sliding failure is not taken into consideration in the design. The demand parameter for this fragility group is the story-drift ratio. However, in a multi-story cantilever wall, much of the story drift of an upper-story wall component can be caused by the rigid-body rotation induced by the flexural deformation in the lower stories. This rigid-body rotation should be removed from the numerical result not to over-estimate the flexural demand on the wall component. This requires a demand parameter different from the story-drift directly obtained from the analysis. For this reason, a

third demand parameter called modified story-drift ratio has been included in addition to the story drift and floor acceleration. Note that the story-drift ratio is still needed for the gravity frames and non-structural components. To use this third demand parameter in the loss assessment, the fragility group B1052.004 has to be modified in the fragility manager to use a new demand parameter, as shown in Figure 1-9. Once this is done, the fragility group B1052.004 is included and the new demand parameter appears automatically.

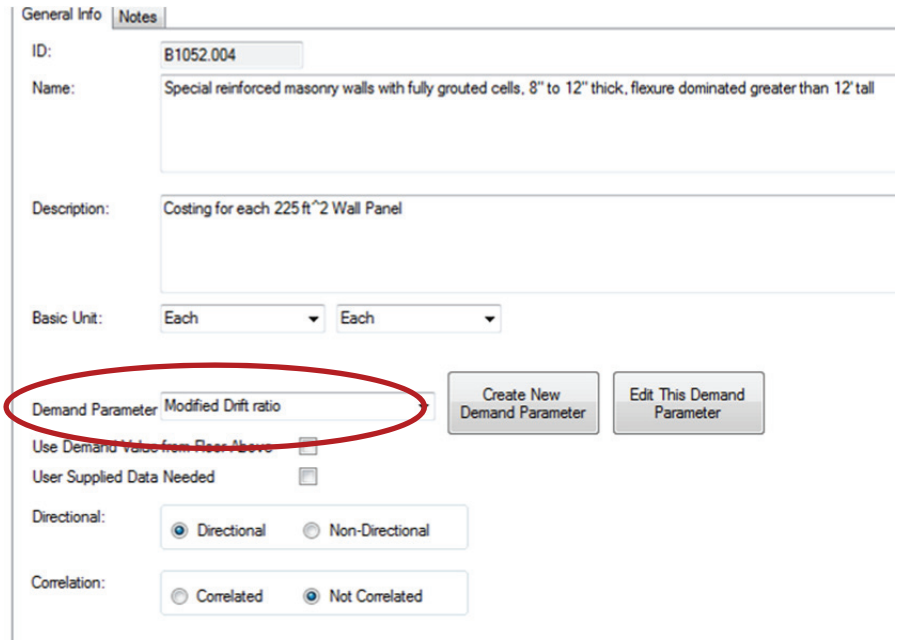

Figure 1-9 Modification of demand parameter for masonry shear wall fragility group

Exterior non-structural elements

The following fragility groups have been selected to represent the exterior non-structural elements of the building.

- The building envelope is represented by *B1071.002 Light framed wood walls with structural panel sheathing, stucco, hold-downs*. This fragility group is included in the first and second levels of the building and applied to directions 1 and 2.
- Windows are represented by *B2022.001a: Glazing – Annealed Monolithic - 6:5 aspect ratio (H:W) - Frame Clearance: 0.43 in. (11mm) - Glass Thick (inner): 1/4 in. (6mm) - Glass Thick (outer):none.* They are included in the first and second levels of the building and applied to directions1 and 2.

- The roof is represented by *B3011.011 Concrete tile roof, tiles secured and compliant with UBC 94.* This fragility group is included in the third level of the building and it is non-directional.

Interior non-structural elements

The following fragility groups have been selected to represent the interior non-structural elements of the building.

- Interior partitions are included in levels 1 and 2 in both directions using the following two fragility groups:
  - *C1011.001a: Wall Partition, Type: Gypsum, Full Height, Fixed Below, Fixed Above.*
  - *C3011.002c: Wall Partition, Type: Gypsum + Ceramic Tile, Full Height, Fixed Below, Slip Track Above w/ returns (friction connection).*
- Suspended ceilings are included in levels 1 and 2 as non-directional using fragility group *C3032.003a: Suspended Ceiling, SDC D,E (Ip=1.0), Area (A): A < 250, Vert & Lat support.* For damage assessment, the performance group located on floor *i* will be subjected to the acceleration at floor *i*+1. This is considered in PACT by selecting the option "Use Demand Value from Floor Above" in the Fragility Manager.
- A staircase is included in levels 1 and 2 as a non-directional element using fragility group *C2011.021a: Stair - cast in place concrete, with seismic joint, replace with cast in place concrete.* This fragility group is directional by default but has been changed to non-directional in the Fragility Manager. It is reasonable to consider that the staircase can be damaged by shaking in either direction of the building. However, placing this fragility group in both directions would double-count the potential damage, and it cannot be distributed between the two directions because there is only one unit per story. For this reason, it has been assumed as non-directional.

Services

The following fragility groups have been selected for service components in the building.

- One elevator is included and represented by fragility group *D1014.010: Traction elevator.* It is assigned only to level 1 and it is non-directional.
- Cold water piping and sanitary waste piping are included in levels 1 and 2 as non-directional and are represented by the following piping and bracing fragility groups, respectively.

- *D2021.013a: Domestic Cold Water Piping (dia > 2.5 inches), SDC D,E,F, PIPING FRAGILITY*
- *D2021.013b: Domestic Cold Water Piping (dia > 2.5 inches), SDC D,E,F, BRACING FRAGILITY*
- *D2031.013b: Sanitary Waste Piping - Cast Iron w/flexible couplings, SDC D,E,F, BRACING FRAGILITY*

- An HVAC system is included in levels 1 and 2 as non-directional using the following fragility groups:
  - *D3041.021c: HVAC Stainless Steel Ducting less than 6 sq. ft in cross sectional area, SDC D, E, or F*
  - *D3041.032c: HVAC Drops / Diffusers without ceilings - supported by ducting only - No independent safety wires, SDC D, E, or F*
- Hot water piping and heating water piping are included in levels 1 and 2 as non-directional. The same piping and bracing fragility groups are used for both piping systems:
  - *D3044.013a: Domestic Hot Water Piping - Small Diameter Threaded Steel - (2.5 inches in diameter or less), SDC D, E, or F, PIPING FRAGILITY*
  - *D3044.013b: Domestic Hot Water Piping - Small Diameter Threaded Steel - (2.5 inches in diameter or less), SDC D, E, or F, BRACING FRAGILITY*
  - *D3044.023a: Domestic Hot Water Piping - Large Diameter Welded Steel - (greater than 2.5 inches in diameter), SDC D, E, or F, PIPING FRAGILITY*
  - *D3044.023b: Domestic Hot Water Piping - Large Diameter Welded Steel - (greater than 2.5 inches in diameter), SDC D, E, or F, BRACING FRAGILITY*
- Fire sprinklers are included in levels 1 and 2 as non-directional using the following fragilities:
  - *D4011.013a: Fire Sprinkler Water Piping - Horizontal Mains and Branches - New Style Vitaulic / Threaded Steel, SDC D, E, or F, PIPING FRAGILITY*
  - *D4011.013b: Fire Sprinkler Water Piping - Horizontal Mains and Branches - New Style Vitaulic / Threaded Steel, SDC D, E, or F, BRACING FRAGILITY*

- *D4011.033a: Fire Sprinkler Drop Standard Threaded Steel - Dropping into unbraced lay-in tile SOFT ceiling - 6 ft. long drop maximum, SDC D, E, or F*

- Electrical equipment is included as non-directional (even though it is considered directional by default) using the following fragility groups:
- D5011.013g: Transformer/primary service - Capacity: 350 to <750 kVA - Equipment that is either hard anchored or is vibration isolated with seismic snubbers/restraints - Anchorage fragility only (included in level 1 only).
- D5011.013h: Transformer/primary service - Capacity: 350 to <750 kVA - Equipment that is either hard anchored or is vibration isolated with seismic snubbers/restraints - Equipment fragility only (included in level 1 only).
- D5012.023d: Low Voltage Switchgear - Capacity: 350 to <750 Amp - Equipment that is either hard anchored or is vibration isolated with seismic snubbers/restraints - Anchorage fragility only (included in levels 1 and 2).
- D5012.023e: Low Voltage Switchgear - Capacity: 350 to <750 Amp - Equipment that is either hard anchored or is vibration isolated with seismic snubbers/restraints - Equipment fragility only (included in levels 1 and 2).
- D5012.033d: Distribution Panel - Capacity: 350 to <750 Amp - Equipment that is either hard anchored or is vibration isolated with seismic snubbers/restraints - Anchorage fragility only (included in level 1 only).
- D5012.033e: Distribution Panel - Capacity: 350 to <750 Amp - Equipment that is either hard anchored or is vibration isolated with seismic snubbers/restraints - Equipment fragility only (included in level 1 only).

It should be noted that all piping, HVAC, and sprinklers supplying floor *i* are attached to the ceiling. For damage assessment, the performance group located on floor *i* will be subjected to the acceleration at floor *i*+1. This is considered in PACT by selecting the option "Use Demand Value from Floor Above" in the Fragility Manager.

The reason to change the electrical equipment from directional to non-directional is the same as that for the staircase. It is assumed that this equipment can be damaged by shaking in either direction of the building.

However, placing it in both directions would double-count the potential damage, and it cannot be distributed between the two directions because it has been assumed that there is only one unit per floor. For this reason, it is preferable to treat it as non-directional.

For electrical systems anchorage (D5011.013g, D5012.023d, D5012.033d), the user needs to provide parameters defining the probability distribution that relates floor acceleration to damage. In all cases, the median has been assumed to be 2g and the dispersion is 0.5, based on the consensus reached by the Beta Testing team.

Entertainment equipment

The following fragility group has been selected to represent entertainment equipment inside the building.

- TV sets are included in levels 1 and 2 as non-directional using fragility group *E2022.020: Home entertainment equipment, unknown installation.*

Performance Groups Tab

In this tab, the aforementioned fragility groups are automatically subdivided into performance groups according to the level (1, 2 or 3) the components are located and the direction (1, 2, or non-directional) to which it is relevant. The quantity of the non-structural components corresponding to each performance group has been determined based on the geometry and square footage of the building using the normative quantities provided in the ATC-58 Guidelines. The normative quantities considered here are the 50% percentile values defined for hospitality-type buildings. No dispersion has been assumed for any of the quantities.

All performance groups are assumed to have correlated damage within each group to reduce the computational effort required (see sensitivity analysis in Section 1.1.7 for more information). The demand parameter associated with each performance group depends on the fragility group. In this case, all directional performance groups have the story-drift ratio as the demand parameter and almost all non-directional performance groups (except stairs, which use drift ratio) use floor acceleration as the demand parameter. The masonry shear walls use the modified story drift as demand parameter. As an example, the input information for performance groups in level 2 and direction 1 is presented in Figure 1-10.

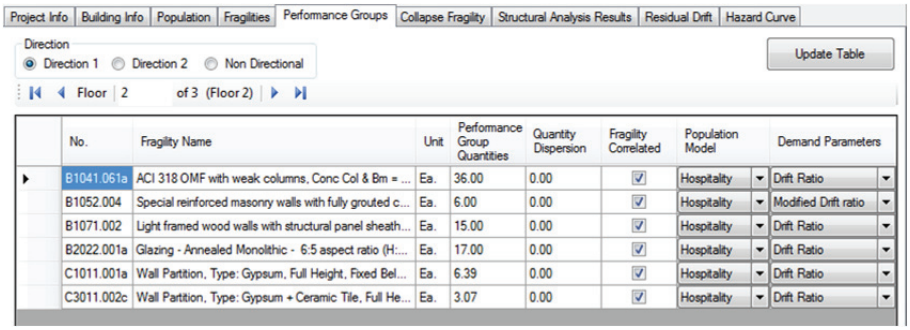

	No.	Fragility Name	Unit	Performance Group Quantities	Quantity Dispersion	Fragility Correlated	Population Model	Demand Parameters
▸	B1041.061a	ACI 318 OMF with weak columns, Conc Col & Bm = ...	Ea.	36.00	0.00	☑	Hospitality	Drift Ratio
	B1052.004	Special reinforced masonry walls with fully grouted c...	Ea.	6.00	0.00	☑	Hospitality	Modified Drift ratio
	B1071.002	Light framed wood walls with structural panel sheath...	Ea.	15.00	0.00	☑	Hospitality	Drift Ratio
	B2022.001a	Glazing - Annealed Monolithic - 6:5 aspect ratio (H:...	Ea.	17.00	0.00	☑	Hospitality	Drift Ratio
	C1011.001a	Wall Partition, Type: Gypsum, Full Height, Fixed Bel...	Ea.	6.39	0.00	☑	Hospitality	Drift Ratio
	C3011.002c	Wall Partition, Type: Gypsum + Ceramic Tile, Full He...	Ea.	3.07	0.00	☑	Hospitality	Drift Ratio

Figure 1-10 Performance group definition for level 2 and direction 1

Collapse Fragility Tab

For the sake of simplicity, only one collapse mode has been considered in the analysis. The collapse fragility used here assumes a lognormal distribution relating the probability of collapse to the spectral acceleration $S_a(T)$ at the fundamental period of the building. The collapse fragility has been derived following the method proposed in Section 6.3 of the 90% draft of Volume 1 of the ATC-58 Guidelines using the results of nonlinear time history analyses, which have been conducted with a set of 20 pairs of ground motion records scaled to different intensity levels. Details of these analyses will be presented in a later section. Collapse has been defined with the criteria proposed by Koutromanos and Shing (2010) for the ATC-76 study. Collapse in a flexure critical reinforced masonry wall is assumed to occur when either one of the following two conditions is met:

- Excessive crushing in the wall cross section, which is defined as the condition that 30% of the cross section has reached the end of the softening branch of the stress-strain relation for masonry.
- Rupture or buckling of a large portion of the flexural reinforcement, which can be quantified as the condition that 30% or more of the bars at a wall cross section has either lost their tensile resistance due to rupture or reached their residual compressive resistance due to buckling.

The curvature at which either of the aforementioned flexural collapse criteria is first reached has been established from a static pushover analysis. In the nonlinear dynamic analyses, collapse is considered to occur when the maximum wall curvature developed at any of the sections exceeds the established curvature limit.

The probability of collapse at each spectral intensity level is taken to be the percentage of cases that have collapsed in any of the two directions. The probability of collapse is plotted in Figure 1-11 as a function of the spectral acceleration. A lognormal distribution function is selected to fit the data. The

best-fit curve has been determined by tying it to the data at a point near the median and setting the dispersion to 0.6, as recommended in Section 6.3 of the 90% draft of Volume 1 of the ATC-58 report (ATC 2011). As a result, the median of the lognormal distribution is 2.1g. The comparison of the results from the nonlinear analyses and the derived lognormal distribution is shown in Figure 1-11. The collapse fragility function derived here is very similar to that obtained by Koutromanos and Shing (2010) for the ATC-76 study, which is also included in Figure 1-11. They obtained a median of 2.14g and a dispersion 0.525 using a similar nonlinear model but following the FEMA P695 (ATC-63) methodology (ATC 2009).

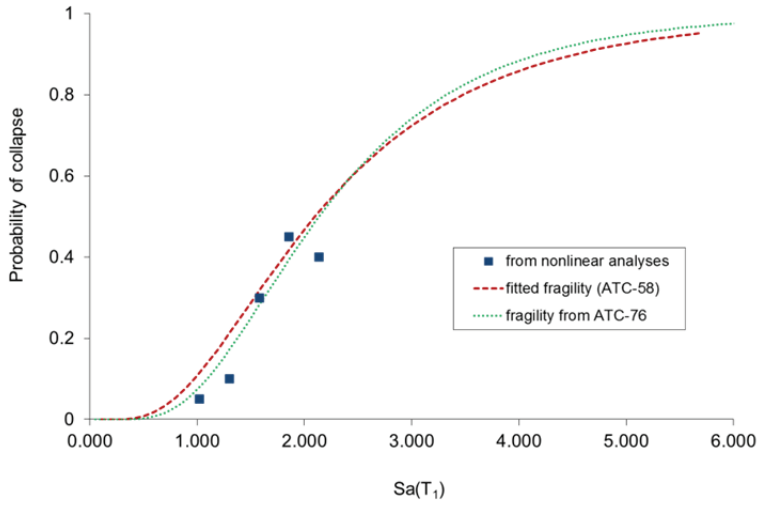

Figure 1-11 Comparison of collapse fragilities

The collapse consequences also need to be defined. For this purpose, it is assumed that 100% of the floor area can be subjected to collapse debris. In terms of casualties, the consequences are quantified with the rates of fatalities and injuries with respect to the number of people present at the time of collapse. The fatality rate is assumed to be 90% and the injury rate is 10% for all floors (no coefficient of variation has been assumed).

Structural Analysis Results Tab

The building has been analyzed as a planar structure in each direction. Two different methods, as described in Section 1.1.3, have been used: (a) nonlinear time-history analysis; and (b) simplified analysis based the method recommended in the ATC-58 Guidelines.

Nonlinear Analysis. As it will be described later, for the assessment performed here, the hazard curve shown in Figure 1-1 is divided into eight intensity levels. Eleven pairs of ground motions have been used for the time-history analysis, and, for each intensity level, the records in each pair are

scaled by the same factor to match the intensity level considered. The peak story drift, peak modified story drift, and peak acceleration obtained for each level and direction of the structure are the demand parameters entered in PACT. The demand for a non-directional component is computed automatically by taking the maximum demand of the two directions multiplied by a factor that is assumed to be 1.2. Results corresponding to collapse situations have been ignored. Since collapse is already accounted for by the collapse fragility, keeping the demand vectors associated with a collapse situation will over-estimate the total loss. Since the vectors corresponding to collapse are removed, the number of demand vectors varies for each intensity level.

The modeling dispersion has been determined with equation 5-1 in Volume 1 of the 90% draft of the ATC-58 Guidelines. By assuming an average building definition and construction quality assurance, and an average model quality and completeness, the total modeling dispersion is calculated to be 0.35.

An example of input information on story-drift ratios for intensity level 8 and direction 1 is shown in Figure 1-12. There are 7 demand vectors for this intensity level after those corresponding to a collapse state have been eliminated.

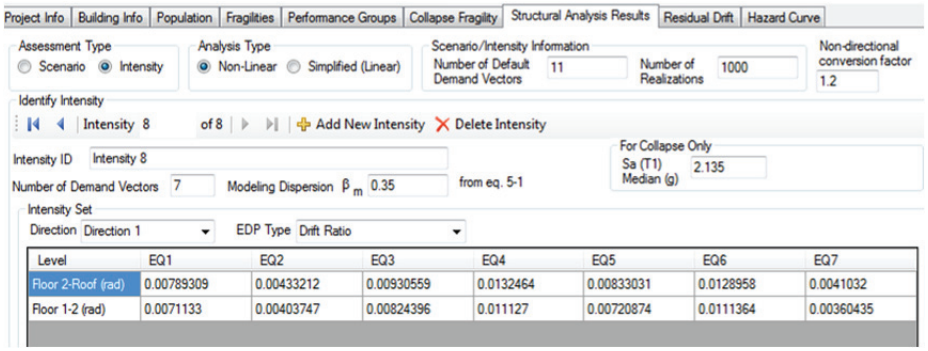

Figure 1-12 Nonlinear analysis results input in PACT

Simplified Analysis. The simplified analysis is also performed for each intensity level for each direction of the building. The story-drift ratios and accelerations obtained from the analysis are taken as the median values. Dispersions are determined with the data given in Table 1-6 of the 90% draft of Volume 1 of the ATC-58 report. The input values on story drifts for intensity level 8 and direction 1 are shown in Figure 1-13.

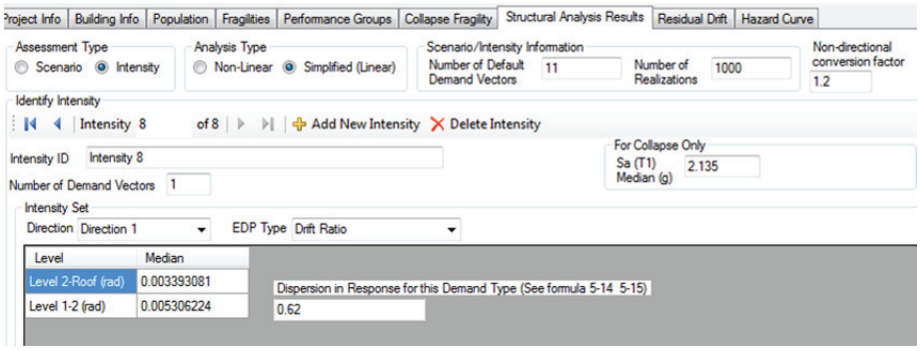

Figure 1-13 Simplified analysis results input in PACT

Residual Drift

The residual drift ratio is used as a demand parameter for the reparability fragility, which determines the probability that the building is not reparable for a given residual drift. The maximum residual story-drift demands for each intensity level and ground motion record have been calculated based on the ATC-58 recommendations. These demands correspond to the residual drifts of the first story, in which structural damage in the RMSW building is expected to concentrate. Instead of using drift values from nonlinear time-history analysis, ATC-58 recommends using the following formula to calculate the residual drift Δ_r.

$$\begin{aligned} \Delta_r &= 0 && \text{for } \Delta \le \Delta_y \\ \Delta_r &= 0.3(\Delta - \Delta_y) && \text{for } \Delta_y < \Delta \le 4\Delta_y \\ \Delta_r &= \Delta - 3.1\Delta_y && \text{for } 4\Delta_y < \Delta \end{aligned}$$

where Δ is the transient peak drift, and Δ_y is the drift at yield. The values of Δ are obtained from nonlinear time-history analysis, and Δ_y is based on a bilinear approximation of the base shear vs. 1st story-drift curve obtained from a nonlinear pushover analysis as shown in Figure 1-14.

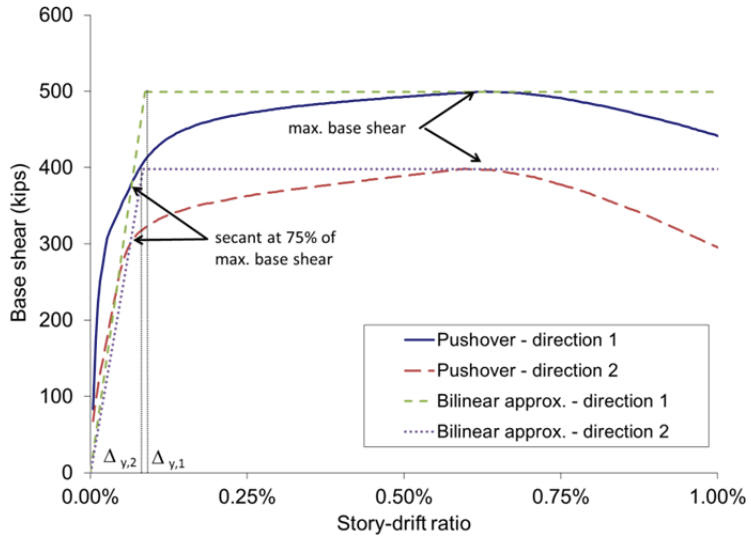

Figure 1-14 Story-drift ratio at yield

The residual drift has been calculated for each direction of the building and the maximum of the two has been taken as the residual drift demand. For the lower intensities, most of the residual drifts are zero. To avoid problems running PACT, zero values have been substituted by artificial low values (see the Section 1.1.10 Appendix on PACT error reports).

The residual drift fragility is defined by a lognormal cumulative distribution function with the median and dispersion set to 1% and 0.3, respectively. These are the default parameters used in PACT for a typical building.

Hazard Curve Tab

The hazard curve for this building site, as described in the PACT Beta Test Overview Report, BD-3.7.13, is input in PACT. The curve has been divided into eight uniform intensity intervals with the boundaries indicated by white circles in Figure 1-15. With this information, PACT creates eight intensity stripes to integrate the intensity-based results to obtain the time-based results.

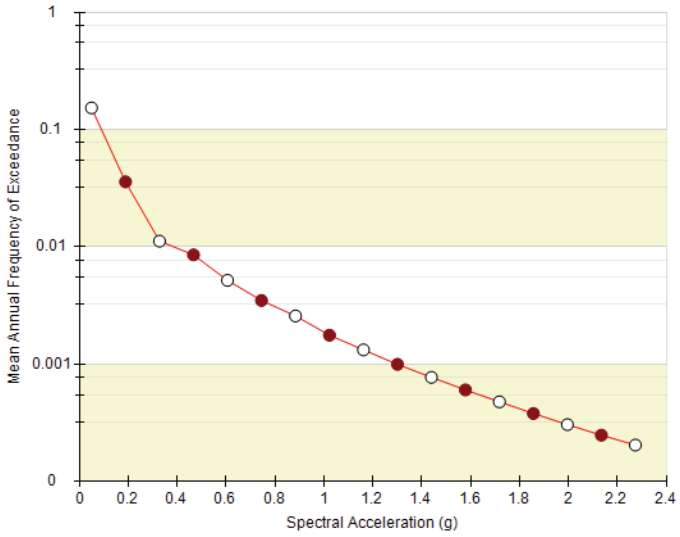

Figure 1-15 Hazard curve

1.1.5 Comparison of Nonlinear and Simplified Analysis Results

The statistical data on the story-drift ratios and floor accelerations obtained from nonlinear time-history and simplified analyses are compared in Figure 1-16 through Figure 1-20. In each plot, the 10th, 50th and 90th percentile values are shown. The values from the nonlinear time-history analysis are based on results from eleven pairs of ground motion records, while the values from the simplified analysis are based on the median and dispersion of the respective demand parameters. These plots show that the simplified analysis underestimates the story-drift ratios in both directions significantly for all stories. They also show that the simplified method tends to give higher floor accelerations on average for the upper intensity levels, and significantly larger dispersions in the acceleration values.

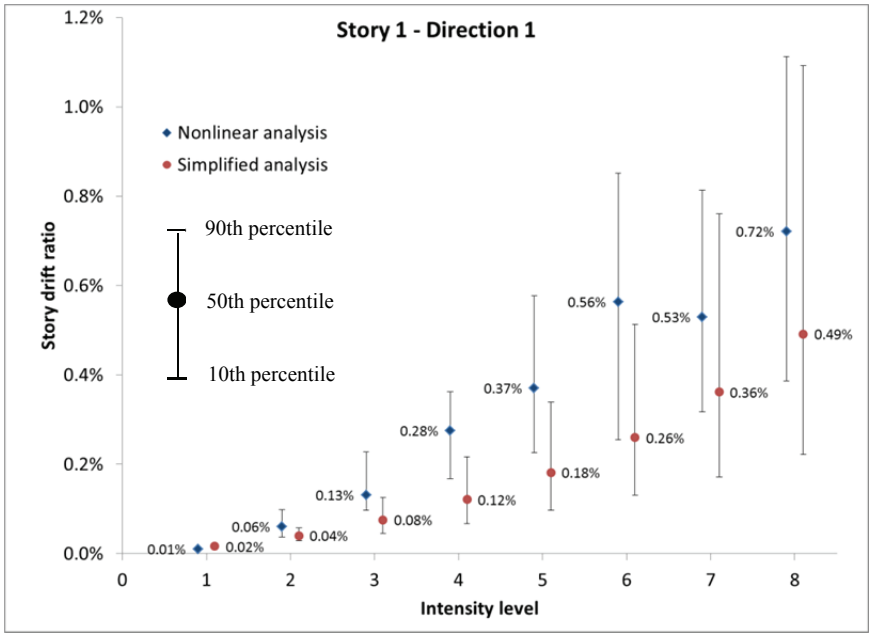

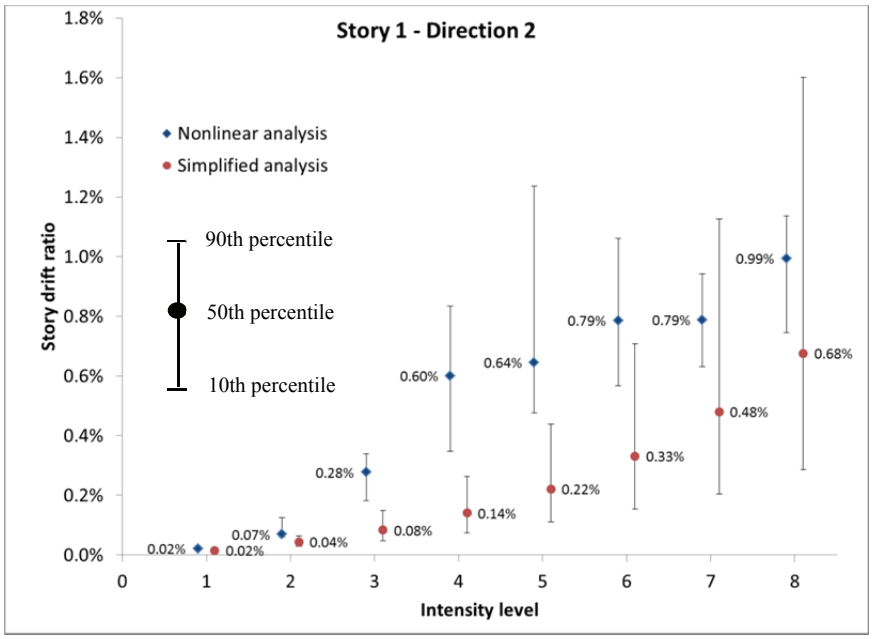

Figure 1-16 Story-drift demands in story 1

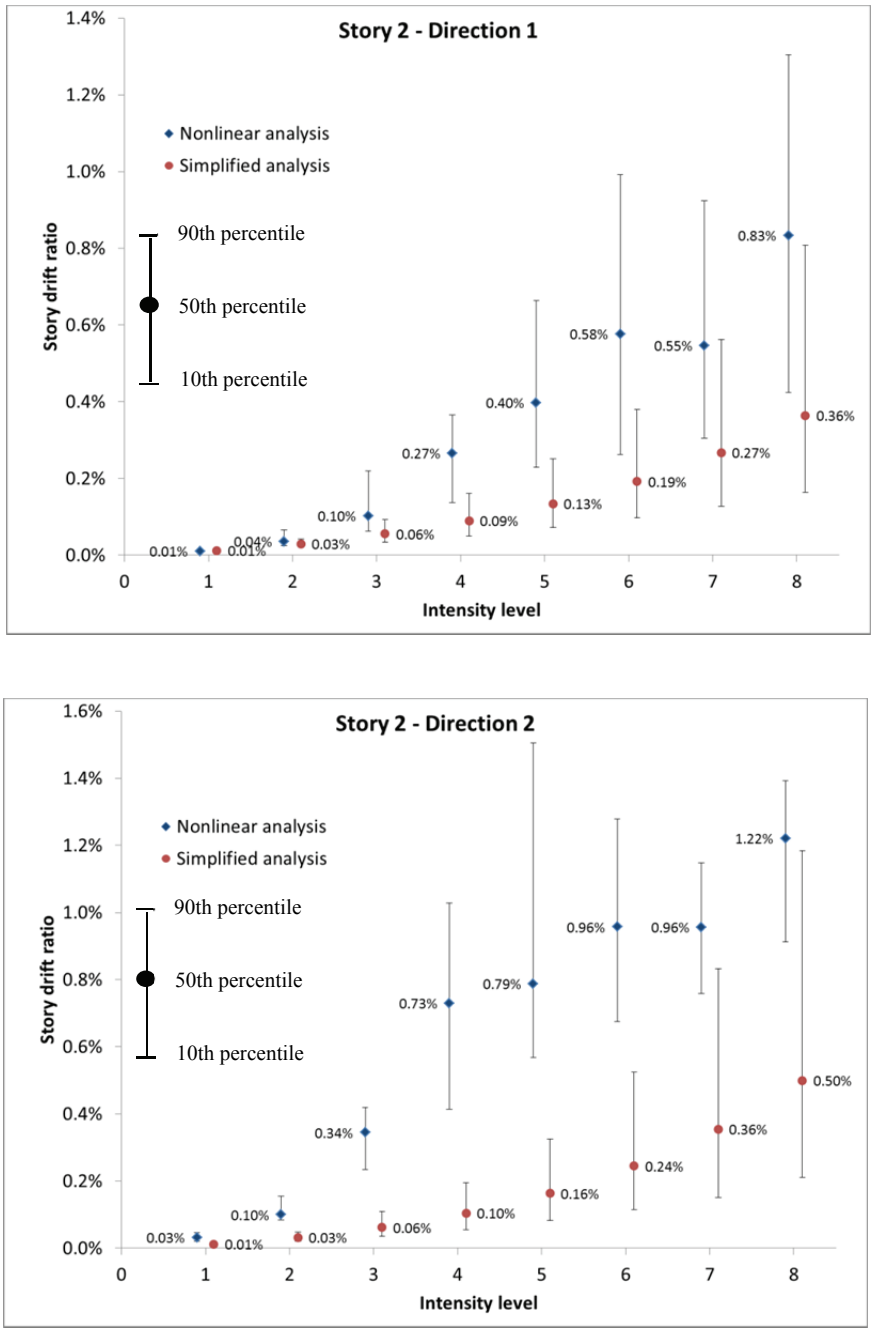

Figure 1-17 Story-drift demands in story 2

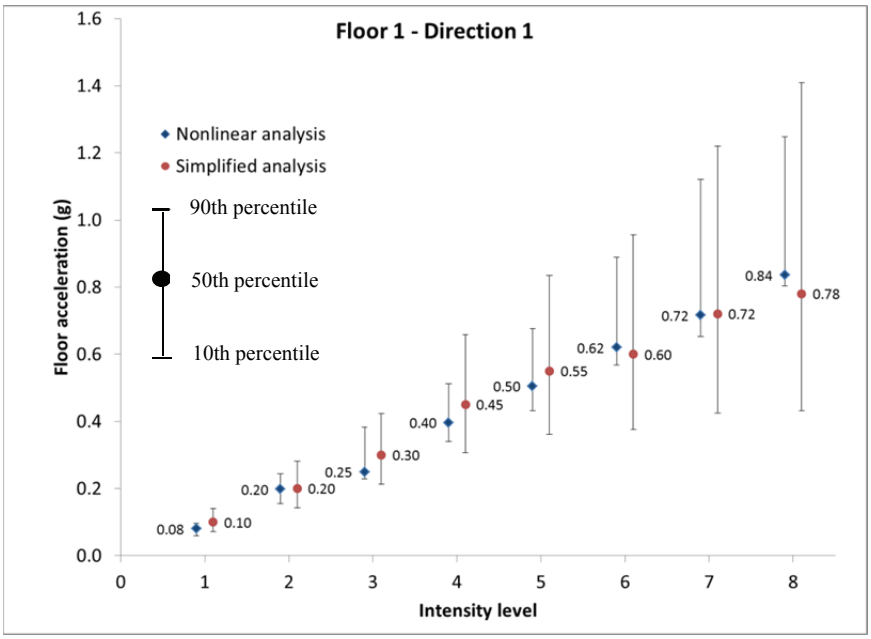

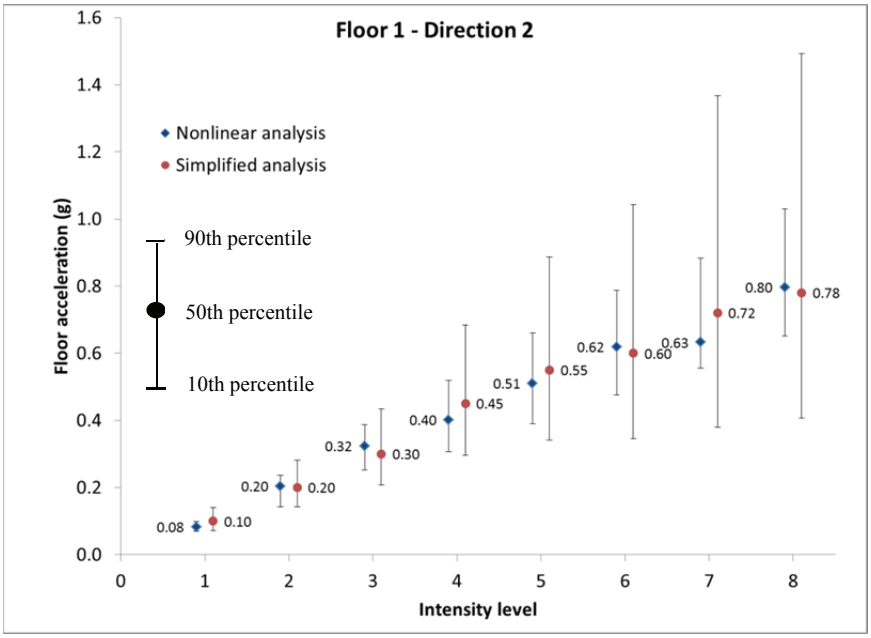

Figure 1-18 Acceleration demands in floor 1

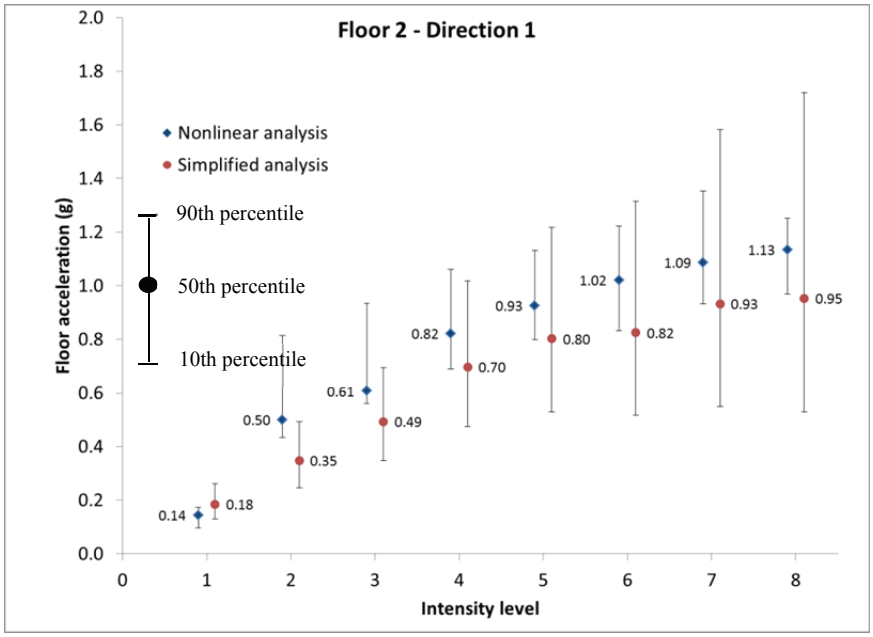

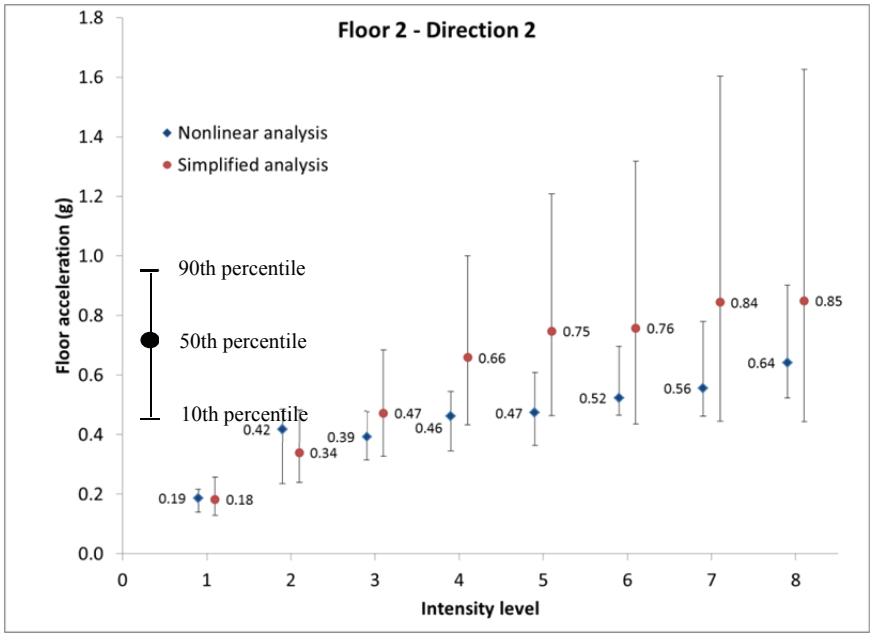

Figure 1-19 Acceleration demands in floor 2

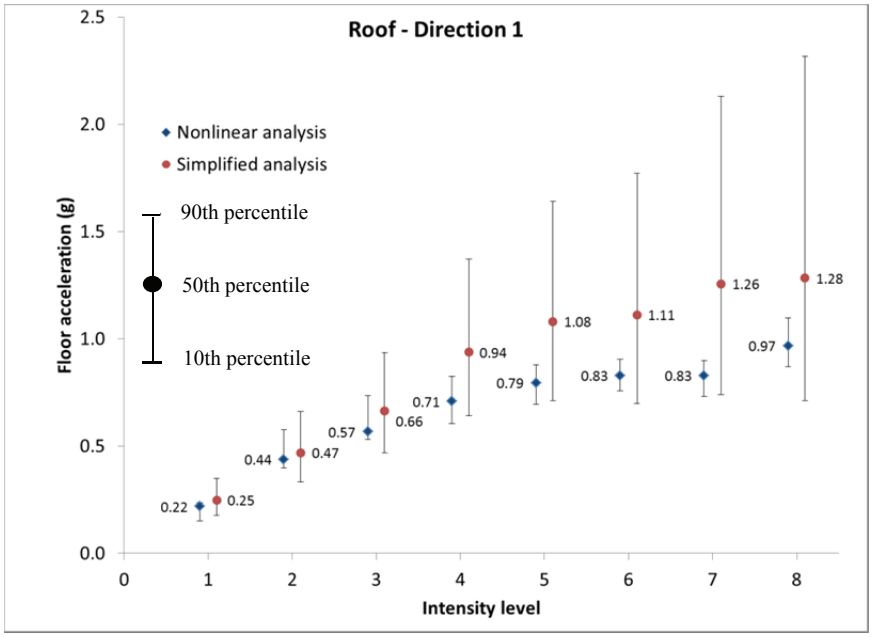

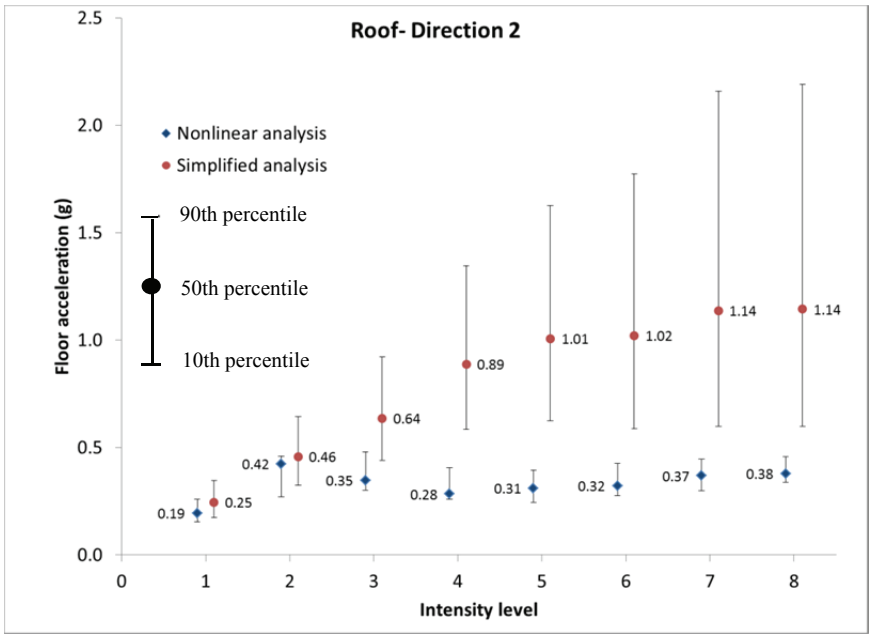

Figure 1-20 Acceleration demands in roof

1.1.6 Loss Predictions for Building

Loss predictions for the building have been conducted using the intensity-based and time-based assessment methods. Two different analytical methods, time history and simplified analysis, have been used to calculate the Engineering Demand Parameters (EDP) for the loss assessments, as described previously, and the resulting loss estimates are compared.

Time-based Results

Results of the time-based analysis are presented in terms of annualized probabilities of collapse and red tagging; and annualized total repair cost, downtime, and number of fatalities and injuries. The downtime is based on a parallel time strategy, i.e., all floors are subjected to repair activities at the same time. Results obtained with nonlinear time-history and simplified analyses are summarized in Table 1-1. They are the average values obtained from 20 runs. Based on a sensitivity study, the number of realizations for each run has been set to 1000. The annualized total values are obtained by integrating the curves of the annual probability of exceedance for the respective quantities. The probability curves from one of the runs are presented in Figure 1-21 through Figure 1-24. The color code shows the contribution of each intensity level to the total value.

Table 1-1 Time-based results

Time-based results	Type of analysis	
	Nonlinear time-history analysis	Simplified analysis
Annualized probability of collapse	0.00071	0.00071
Annualized probability of red tagging	0.0089	0.0036
Annualized total cost ($)	16,615	11,188
Annualized total downtime (days)	0.685	0.456
Annualized total no. of fatalities	0.086	0.083
Annualized total no. of injuries	0.016	0.012

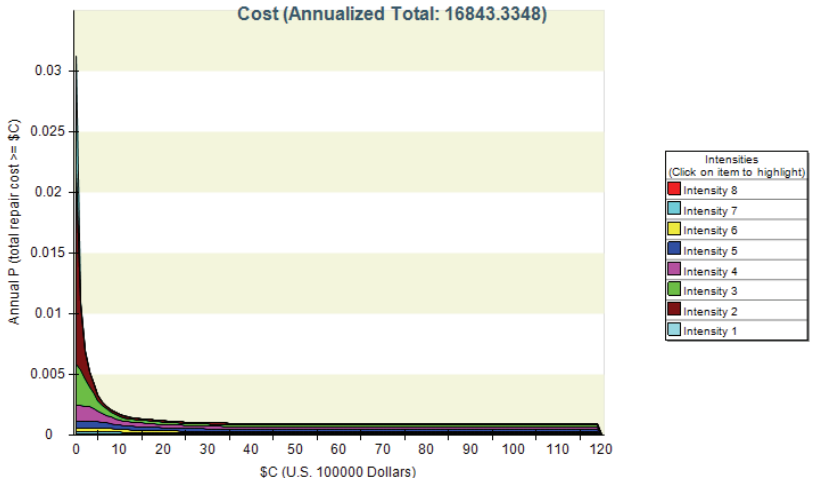

Figure 1-21 Annual probability of exceedance on repair cost

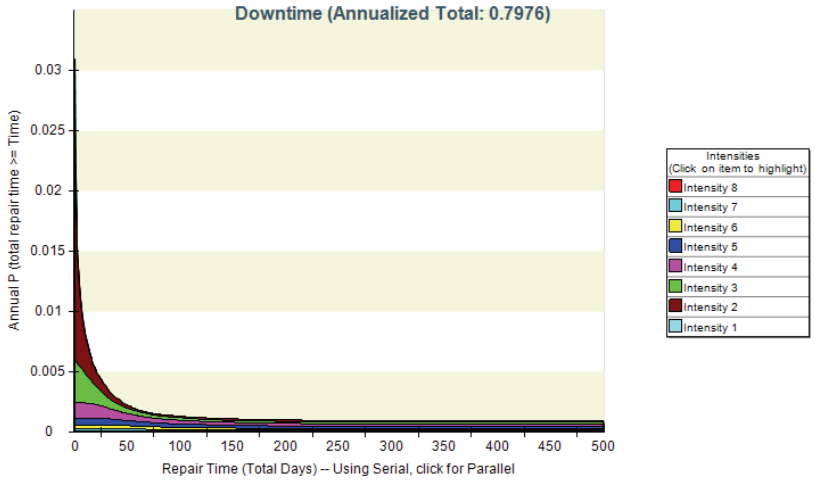

Figure 1-22 Annual probability of exceedance on downtime

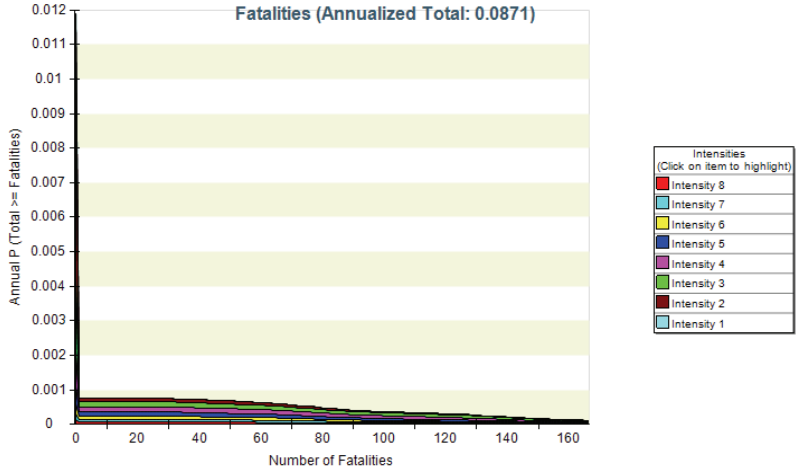

Figure 1-23 Annual probability of exceedance on fatalities

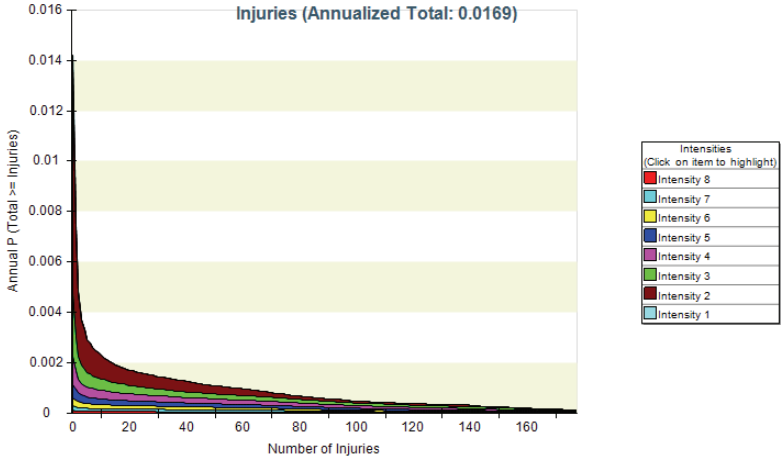

Figure 1-24 Annual probability for exceedance on injuries

The annualized probability of collapse is 0.00071, which corresponds to a collapse return period of approximately 1,400 years. This is a bit high considering the fact that a structure should have a low probability of collapse for an intensity level that has 2% probability of exceedance in 50 years or a return period of 2,475 years. This can be attributed to the relatively high dispersion assumed for the collapse fragility leading to a relatively high probability of collapse for lower intensity levels. This, in turn, results in an elevated annualized number of fatalities (0.086) and injuries (0.016). As it can be observed in Figure 1-21 through Figure 1-24, the low and moderate intensity levels (intensities 2 to 5) have a significant contribution to the annualized losses. This is a result of the combination of a relatively high probability of occurrence of low intensity motions with the high dispersion of the collapse fragility. Collapse realizations occur as early as intensity 2, and the number of collapses increases with the intensity level. The annualized probability of collapse is independent of the structural analysis method used (nonlinear or simplified) since it is determined solely from the collapse fragility curve and a random number generation. Since the probability of having fatalities depends very much on the probability of collapse, it should not change much with the analysis method. However, results for red tagging, annualized cost, downtime and injuries are influenced by the analysis method used, as shown in Table 1-1. When using the simplified method, the probability of red tagging is reduced by more than one half, the annualized total cost and downtime are reduced by 33%, and the annualized number of injuries is reduced by 25%. As explained in a previous section, the simplified analysis method underestimates the peak story-drift demands. Since the residual story drift is calculated with the peak story-drift demand, the residual drift is also underestimated if the simplified method is used. The reduction in the story drift explains the significant reduction of the red tagging probability. It should be noted that the increase of acceleration for the upper intensity levels does not appear to have a strong influence on the probability of red tagging. Results for the repair cost, downtime, and injuries are less sensitive to the analysis method used than the red tagging probability because they are more dominated by collapse than the red tagging.

Intensity-based results

Loss-assessment results for each of the 8 intensity levels considered are presented in terms of the mean, and the 10, 50, and 90% probabilities of non-exceedance of repair cost, downtime, and number of fatalities and injuries. The downtime is based on a parallel time strategy, i.e., all floors are subjected to repair activities at the same time. Two different types of results are presented: results based on data bins and results based on adjusted

lognormal distributions. Results based on data bins are computed by sorting the losses for each realization in an ascending order and assigning the probability of non-exceedance based on this ranked distribution. Results based on data bins and fitted lognormal distribution are presented in Table 1-2 and Table 1-3, respectively, for the case using nonlinear time-history analysis. The results obtained with the simplified analysis method are presented in Table 1-4 and Table 1-5. In addition, the 10th, 50th and 90th percentile results for the main loss indicators obtained from the nonlinear and simplified analyses using the data bins are compared in Figure 1-25 through

Figure 1-28.

As observed from Table 1-2 to Table 1-5 and from Figure 1-25 to

Figure 1-28, the loss in terms of repair cost, downtime, fatalities, and injuries increase with the level of intensity. The repair cost and downtime obtained with the simplified analysis always tend to be lower than those with the nonlinear analysis. The damage for some performance groups is under-estimated by the simplified analysis. This is because the simplified analysis yields lower peak and residual story drifts as compared to the nonlinear time-history analysis, as pointed out previously. The number of deaths is very similar for both methods because it depends mainly on the probability of collapse. The number of injuries increases if the simplified method is used because the higher accelerations obtained with this method trigger more non-structural damage that causes injuries.

Table 1-2 Intensity-based results obtained with nonlinear analysis based on data bins

Int.	Variable	Mean	Probability of Non-Exceedance		
			10%	50%	90%
1	Repair Cost ($)	4,358	- *	- *	12,333
	Downtime (days)	0.31	- *	- *	0.75
	No. of Fatalities	0.00	- *	- *	- *
	No. of Injuries	0.00	- *	- *	- *
2	Repair Cost ($)	194,969	13,876	74,208	259,375
	Downtime (days)	10.71	1.04	5.69	14.29
	No. of Fatalities	0.61	- *	- *	0.78
	No. of Injuries	0.33	- *	0.01	0.38
3	Repair Cost ($)	902,941	84,746	294,253	915,789
	Downtime (days)	45.13	2.24	11.78	40.45
	No. of Fatalities	4.93	- *	0.23	0.90
	No. of Injuries	0.96	- *	0.07	1.88
4	Repair Cost ($)	2,646,843	329,545	711,111	11,939,394
	Downtime (days)	125.31	11.31	28.65	493.90
	No. of Fatalities	13.41	- *	0.44	63.49
	No. of Injuries	2.20	- *	0.17	8.45
5	Repair Cost ($)	4,583,670	525,882	1,481,818	11,967,742
	Downtime (days)	210.02	17.60	60.38	496.77
	No. of Fatalities	22.47	0.01	0.58	99.50
	No. of Injuries	3.31	0.02	0.37	11.70
6	Repair Cost ($)	5,741,077	700,000	2,450,000	11,975,309
	Downtime (days)	259.43	26.13	100.95	497.53
	No. of Fatalities	31.58	0.07	0.70	123.33
	No. of Injuries	4.61	0.06	1.33	14.50
7	Repair Cost ($)	6,837,841	747,727	11,902,153	11,980,431
	Downtime (days)	301.04	27.82	490.22	498.04
	No. of Fatalities	47.04	0.11	0.87	152.16
	No. of Injuries	6.00	0.07	3.25	16.93
8	Repair Cost ($)	8,337,682	1,188,889	11,920,635	11,984,127
	Downtime (days)	365.36	45.35	492.06	498.41
	No. of Fatalities	56.82	0.16	31.80	163.33
	No. of Injuries	7.18	0.11	5.97	18.23

* The probability of no loss is higher than the percentile indicated.

Table 1-3 Intensity-based results obtained with nonlinear analysis based on adjusted lognormal distribution

Int.	Variable	Mean	Probability of Non-Exceedance		
			10%	50%	90%
1	Repair Cost ($)	4,358	0.007	1	223
	Downtime (days)	0.29	0.05	0.17	0.64
	No. of Fatalities	0.00	0.0004	0.0008	0.001
	No. of Injuries	0.00	0.0006	0.001	0.003
2	Repair Cost ($)	310,419	5,449	57,398	604,656
	Downtime (days)	10.05	0.36	2.81	21.74
	No. of Fatalities	0.61	0.01	0.14	1.25
	No. of Injuries	0.04	0.001	0.01	0.08
3	Repair Cost ($)	592,416	65,153	295,441	1,339,699
	Downtime (days)	23.25	2.39	11.22	52.70
	No. of Fatalities	1.55	0.001	0.04	1.28
	No. of Injuries	1.26	0.01	0.16	2.17
4	Repair Cost ($)	1,522,551	148,047	715,330	3,456,309
	Downtime (days)	64.22	5.54	28.45	145.98
	No. of Fatalities	1.55	0.001	0.04	1.28
	No. of Injuries	1.26	0.01	0.16	2.17
5	Repair Cost ($)	3,332,123	291,872	1,486,832	7,574,102
	Downtime (days)	143.70	11.14	60.31	326.44
	No. of Fatalities	9.76	0.001	0.06	3.66
	No. of Injuries	3.63	0.02	0.37	5.74
6	Repair Cost ($)	5,069,528	511,571	2,425,295	11,498,025
	Downtime (days)	220.08	20.39	101.00	500.00
	No. of Fatalities	36.84	1.E-03	0.09	7.57
	No. of Injuries	10.39	0.10	1.32	17.82
7	Repair Cost ($)	24,902,869	2,550,581	12,000,000	- **
	Downtime (days)	1091.81	100.78	500.00	- **
	No. of Fatalities	117.56	0.001	0.14	15.69
	No. of Injuries	14.60	0.22	3.29	30.06
8	Repair Cost ($)	19,412,096	3,414,236	12,000,000	- **
	Downtime (days)	832.59	137.06	500.00	- **
	No. of Fatalities	123.25	0.27	31.57	261.73
	No. of Injuries	14.36	0.48	5.96	32.60

** The lognormal distribution would give a value that is higher than the maximum possible, and therefore unrealistic. For repair cost, this maximum value is the replacement cost ($12,000,000), and, for downtime, this is the replacement time (500 days).

Table 1-4 Intensity-based results obtained with simplified analysis based on data bins

Int.	Variable	Mean	Probability of Non-Exceedance		
			10%	50%	90%
1	Repair Cost ($)	656	- *	- *	810
	Downtime (days)	0.06	- *	- *	0.07
	No. of Fatalities	0.00	- *	- *	- *
	No. of Injuries	0.00	- *	- *	- *
2	Repair Cost ($)	105,260	7,059	49,840	92,620
	Downtime (days)	4.94	0.65	4.91	9.18
	No. of Fatalities	0.59	- *	- *	0.01
	No. of Injuries	0.08	- *	- *	0.04
3	Repair Cost ($)	552,687	14,728	73,638	226,667
	Downtime (days)	25.30	1.16	5.81	15.27
	No. of Fatalities	4.31	- *	- *	0.82
	No. of Injuries	0.59	- *	0.02	0.22
4	Repair Cost ($)	1,612,713	106,731	247,807	11,913,793
	Downtime (days)	73.04	2.09	10.86	491.38
	No. of Fatalities	13.23	- *	0.35	64.00
	No. of Injuries	2.04	0.01	0.17	8.23
5	Repair Cost ($)	2,965,834	224,074	447,059	11,954,751
	Downtime (days)	131.79	6.90	19.83	495.48
	No. of Fatalities	23.97	- *	0.57	112.33
	No. of Injuries	3.72	0.05	0.63	12.87
6	Repair Cost ($)	4,171,971	336,275	655,357	11,968,354
	Downtime (days)	183.02	12.07	29.55	496.84
	No. of Fatalities	34.33	3.E-03	0.68	137.00
	No. of Injuries	4.71	0.07	1.00	15.35
7	Repair Cost ($)	5,916,370	565,714	1,712,500	11,977,778
	Downtime (days)	258.46	21.55	80.67	497.78
	No. of Fatalities	43.34	0.09	0.83	142.00
	No. of Injuries	6.06	0.18	3.76	15.97
8	Repair Cost ($)	7,845,796	848,718	11,918,434	11,983,687
	Downtime (days)	338.59	32.59	491.84	498.37
	No. of Fatalities	55.62	0.22	6.31	17.72
	No. of Injuries	7.34	0.15	31.71	159.00

* The probability of no loss is higher than the percentile indicated.

Table 1-5 Intensity-based results obtained with simplified analysis based on adjusted lognormal distribution

Int.	Variable	Mean	Probability of Non-Exceedance		
			10%	50%	90%
1	Repair Cost ($)	656	1	20	592
	Downtime (days)	0.06	0.01	0.04	0.13
	No. of Fatalities	0.00008	0.00005	0.00007	0.0001
	No. of Injuries	0.0001	0.00006	0.00009	0.0001
2	Repair Cost ($)	108,316	580	9,695	161,937
	Downtime (days)	1.54	0.09	0.57	3.48
	No. of Fatalities	0.59	0.05	0.27	1.35
	No. of Injuries	0.08	0.01	0.03	0.19
3	Repair Cost ($)	165,794	13,266	70,699	376,774
	Downtime (days)	8.17	0.62	3.40	18.55
	No. of Fatalities	4.31	0.03	0.45	6.85
	No. of Injuries	0.06	0.0004	0.01	0.10
4	Repair Cost ($)	622,192	40,130	237,571	1,406,427
	Downtime (days)	29.89	1.75	10.84	67.26
	No. of Fatalities	1.20	0.0009	0.03	0.97
	No. of Injuries	1.59	0.01	0.15	2.45
5	Repair Cost ($)	1,327,488	64,600	436,696	2,952,063
	Downtime (days)	60.74	2.87	19.67	134.76
	No. of Fatalities	10.09	0.0009	0.06	3.48
	No. of Injuries	6.04	0.04	0.62	9.56
6	Repair Cost ($)	2,028,523	96,098	657,726	4,501,675
	Downtime (days)	93.54	4.17	29.35	206.55
	No. of Fatalities	37.45	0.0009	0.08	7.01
	No. of Injuries	8.33	0.07	0.99	13.96
7	Repair Cost ($)	4,325,114	296,353	1,703,993	9,797,752
	Downtime (days)	213.32	13.73	81.38	482.17
	No. of Fatalities	102.55	0.001	0.12	13.61
	No. of Injuries	14.33	0.39	3.76	30.60
8	Repair Cost ($)	24,159,680	2,634,766	12,000,000	- **
	Downtime (days)	1030.81	107.02	500.00	- **
	No. of Fatalities	30250.34	0.28	31.85	- **
	No. of Injuries	24.57	0.76	6.32	- **

** The lognormal distribution would give a value that is higher than the maximum possible, and therefore unrealistic. For repair cost, this maximum value is the replacement cost ($12,000,000), and, for downtime, this is the replacement time (365 days).

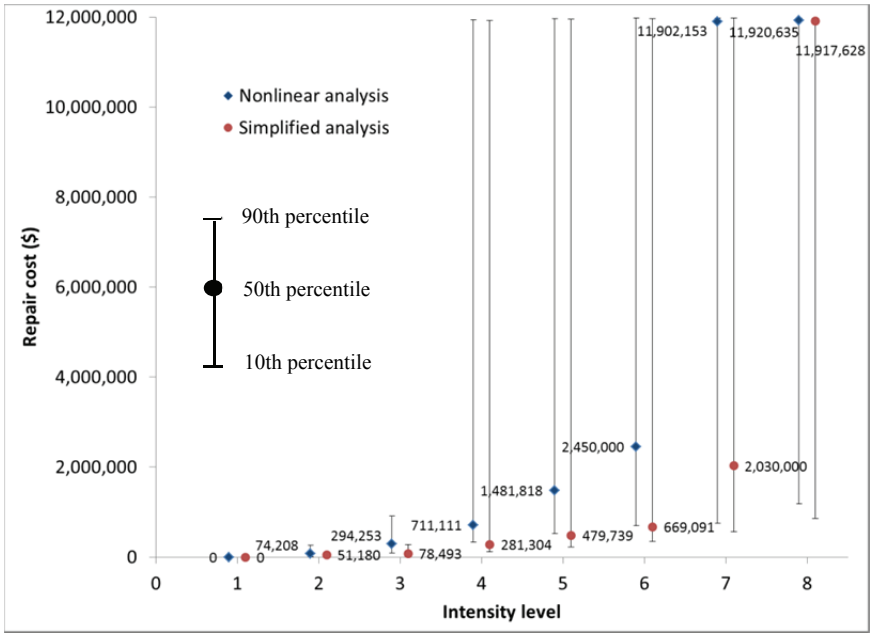

Figure 1-25 Intensity-based results for repair cost

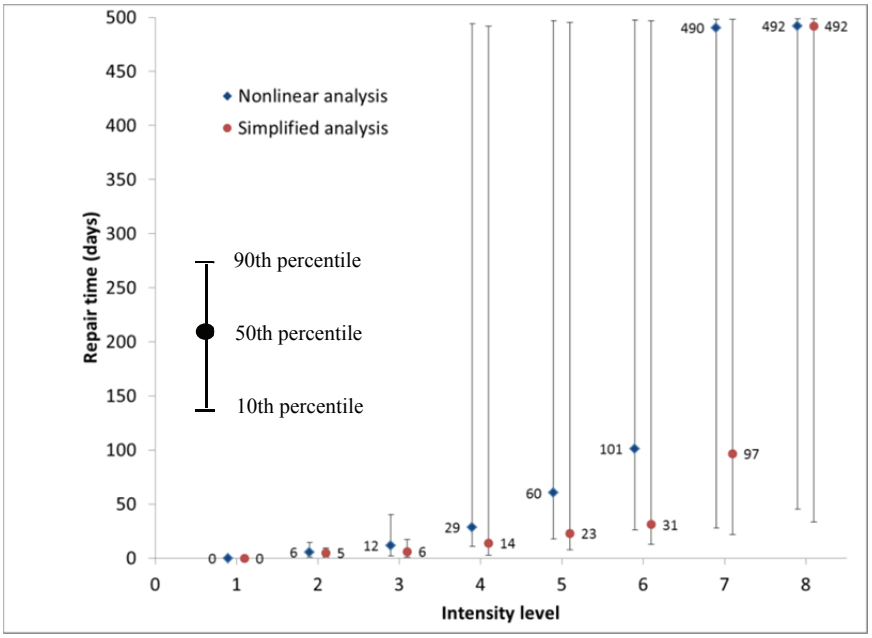

Figure 1-26 Intensity-based results for downtime

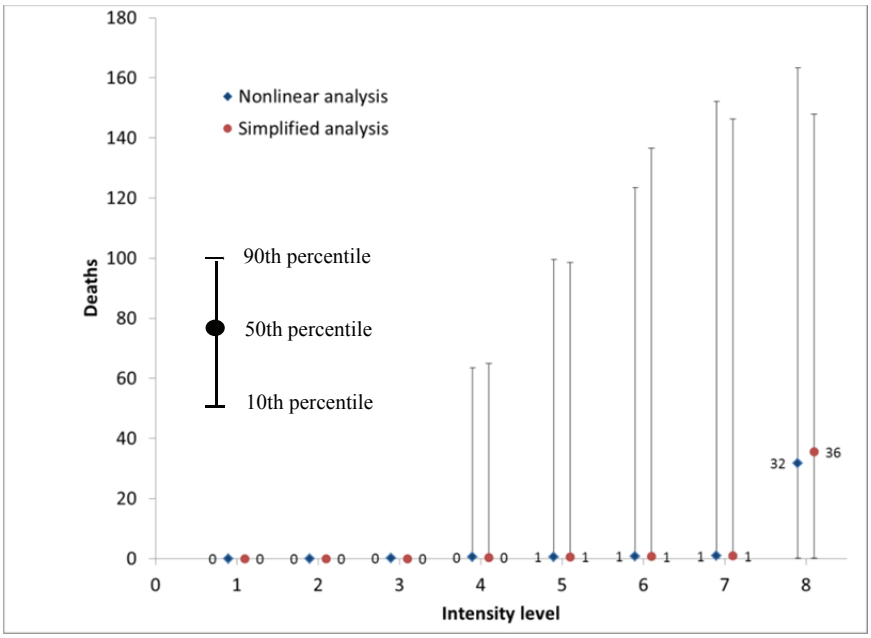

Figure 1-27 Intensity-based results for deaths

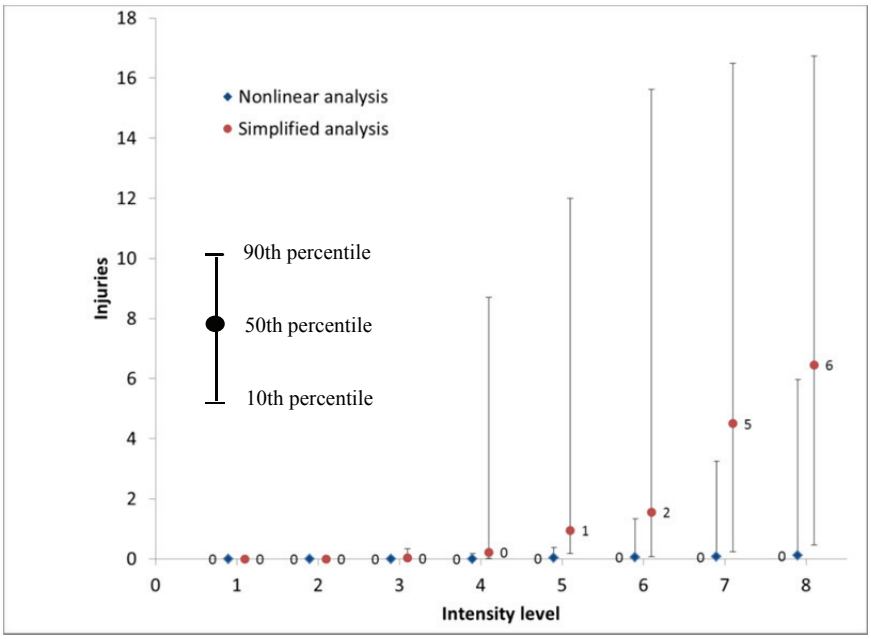

Figure 1-28 Intensity-based results for injuries

The main categories of repair cost have been identified for each intensity level. Figure 1-29 through Figure 1-36 present the repair cost for each realization in one of the runs using nonlinear time-history analysis for the 8 intensity levels. For intensity 1, the losses are mainly damage in the interior components (ceilings and wall finishes). No collapse occurs. The same type of loss is observed for intensity 2, but in this case, a very small number of realizations had collapse. The fact that some realizations result in collapse for such a low intensity level is due to the relatively high dispersion of the collapse fragility. For intensity 3, the cost is mainly contributed by collapse, and damage in the interior components (ceilings and partitions), and structural elements (reinforced concrete frame). The same observation is obtained for intensities 4 and 5, but the losses related to collapse increase and the cost of demolition due to excessive residual drift starts to be important. For intensities 6 to 8, losses related to non-collapse realizations have the same causes, which are damage in interior components, structural damage and demolition due to excessive residual drift, and their costs tend to stabilize, while the overall cost keeps on increasing due to the increase of collapse realizations. For intensity 8, half of the realizations lead to collapse, which represent about two thirds of the total losses for this intensity level.

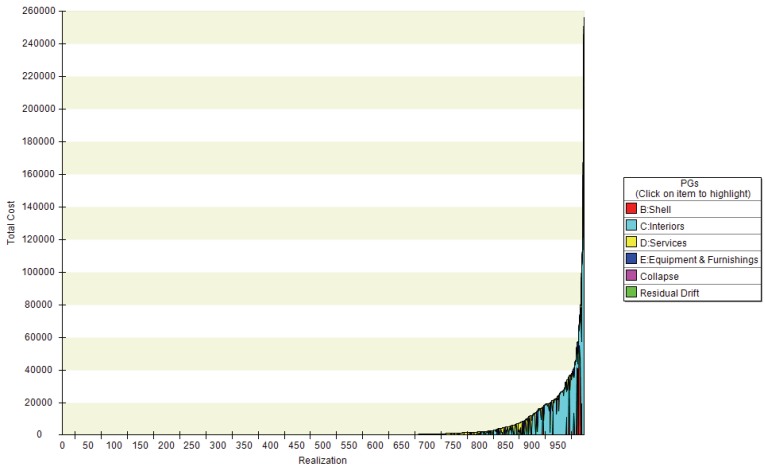

Figure 1-29 Repair cost for each realization at intensity 1

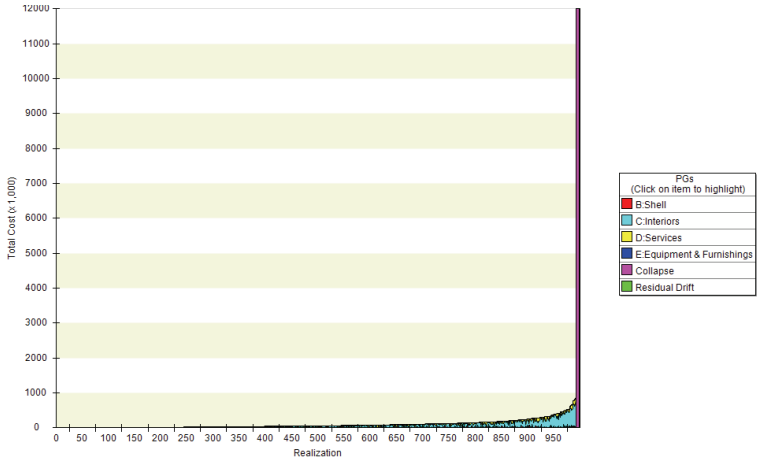

Figure 1-30 Repair cost for each realization at intensity 2

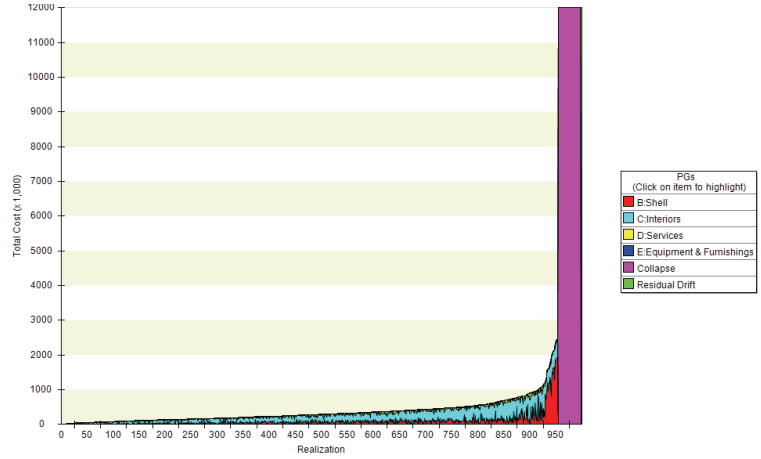

Figure 1-31 Repair cost for each realization at intensity 3

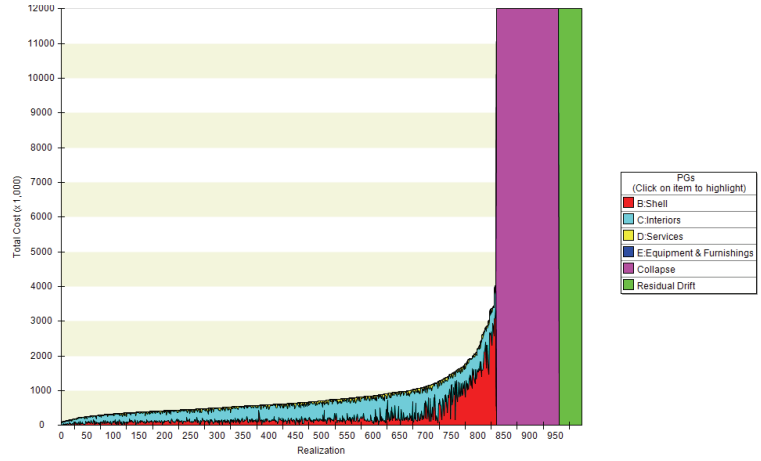

Figure 1-32 Repair cost for each realization at intensity 4

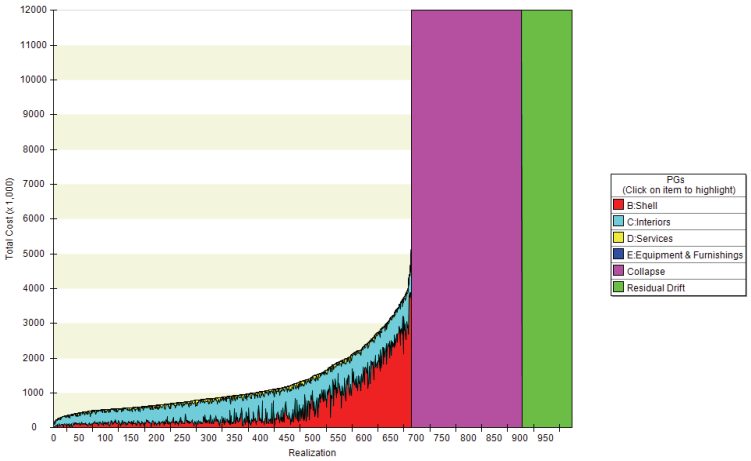

Figure 1-33 Repair cost for each realization at intensity 5

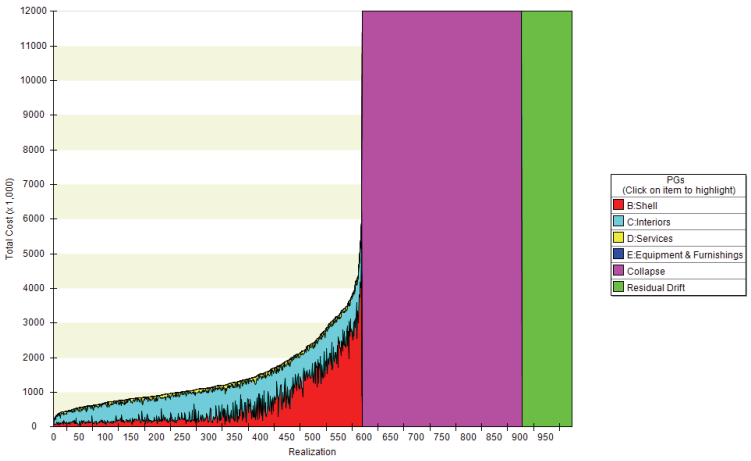

Figure 1-34 Repair cost for each realization at intensity 6

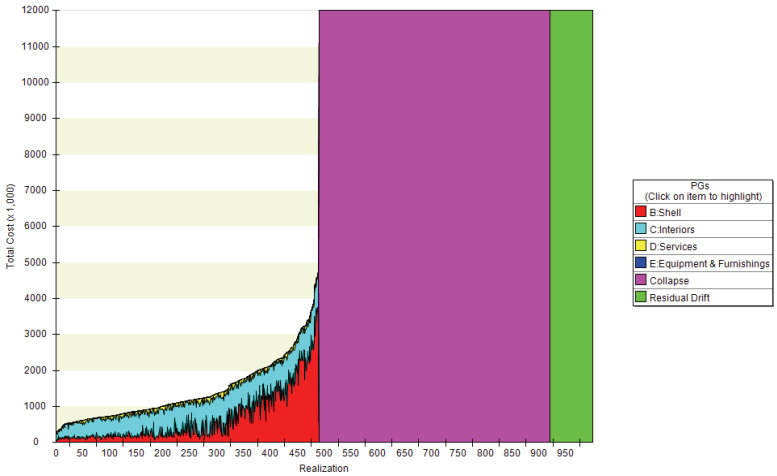

Figure 1-35 Repair cost for each realization at intensity 7

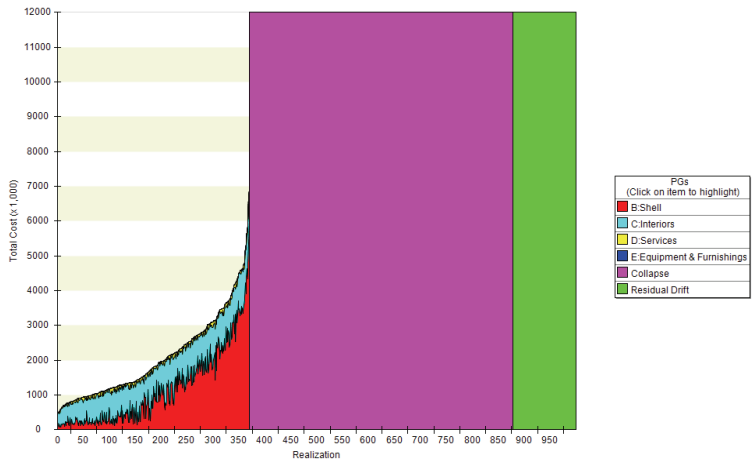

Figure 1-36 Repair cost for each realization at intensity 8

The percentage of realizations resulting in collapse and red tagging for each intensity level are shown in Table 1-6. The percentage of collapses for the lower intensity levels (2 and 3) is not negligible due to the high dispersion of the collapse fragility. Combined with their relatively high probability of occurrence, the lower intensity levels have a major contribution to the overall probability of collapse (and the number of casualties), as shown in the time-based results. At the highest intensity level, the number of collapses is approximately 50% of all the realizations. This result is consistent with the fact that the spectral acceleration *Sa(T)* at this level is very close to the median of the collapse fragility. The percentage of collapses obtained with nonlinear and simplified analyses is the same because they only depend on the collapse fragility (the small difference can only be attributed to the random number generation). The percentage of red tags obtained with the simplified analysis is smaller, especially for the lower intensity levels, because the story-drift demands are smaller than those obtained with nonlinear time-history analysis. This is consistent with what has been observed in the time-based analysis. To illustrate this point, the breakdown of red tags for intensity 3 obtained with the two analysis methods is shown in Figure 1-37 and Figure 1-38. With nonlinear time-history analysis, red tags are mainly due to damage in exterior walls, roof, stairs, fire sprinklers and collapse. With the simplified analysis, red tags are due to collapse, and damage in exterior walls and fire sprinklers. The probabilities of the last two fragility groups triggering a red tag are smaller with the simplified analysis than with the nonlinear time-history analysis.

Table 1-6 Percentage of realizations leading to collapse and red tagging at each intensity level

Intensity	Nonlinear Analysis		Simplified Analysis	
	% of collapses	% with red tag	% of collapses	% with red tag
1	0.0%	0.8%	0.0%	0.0%
2	0.6%	28.5%	0.7%	4.8%
3	4.3%	61.7%	3.9%	25.3%
4	12.0%	93.3%	11.6%	67.5%
5	21.3%	97.8%	22.0%	86.6%
6	30.8%	99.3%	31.3%	90.3%
7	43.1%	99.6%	41.0%	97.3%
8	50.8%	99.8%	51.3%	99.5%

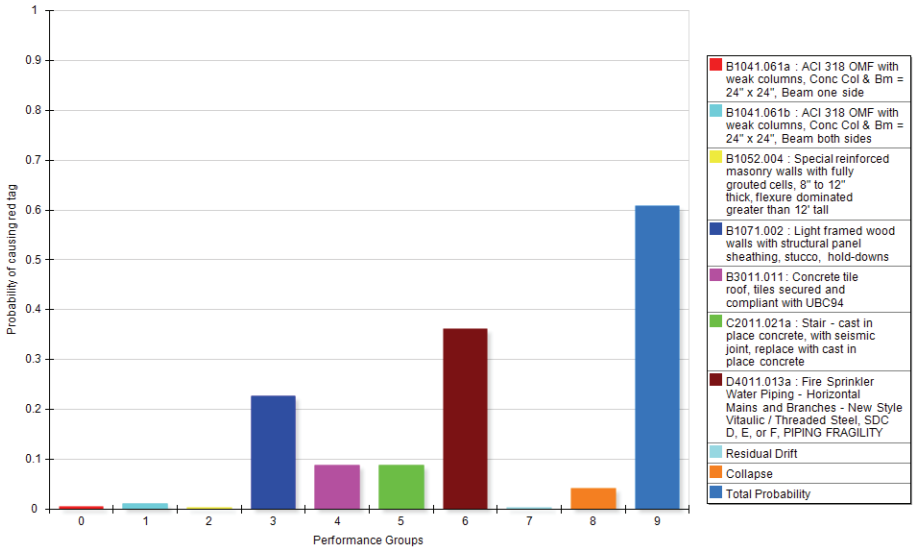

Figure 1-37 Probability of red tagging with nonlinear analysis for intensity 3

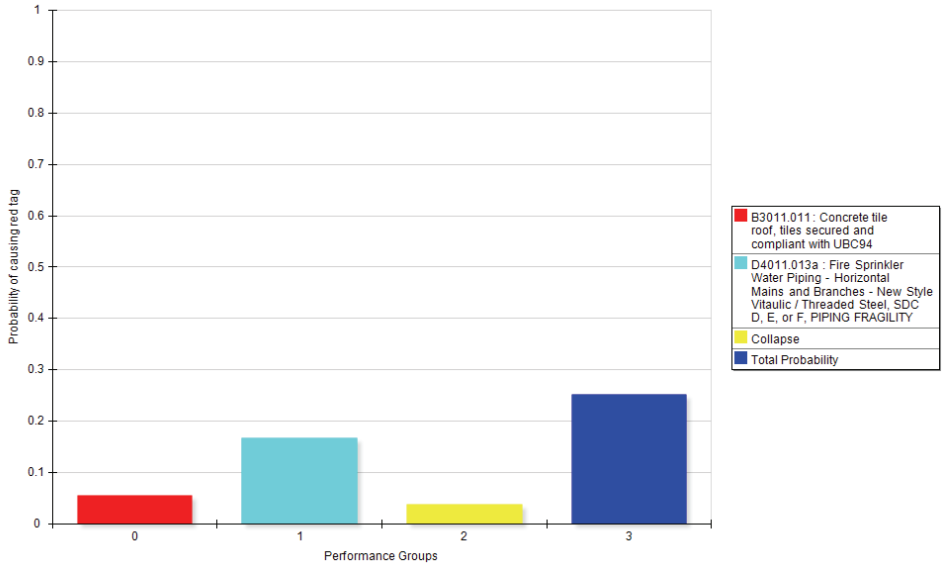

Figure 1-38 Probability of red tagging with simplified analysis for intensity 3

1.1.7 Results of Sensitivity Studies

A number of sensitivity studies have been carried out to investigate the influence of different assumptions in the building model. In all the cases, the loss estimation is based on results from nonlinear time-history analysis. Unless specified otherwise, the time-based results presented in this section are the mean values of the respective time-based results obtained from 5 runs using 1000 realizations each. The intensity-based results presented in this section were obtained in a single run.

Number of realizations

PACT provides loss estimation based on a set of realizations, each of which is triggered by a random number. It is expected that the larger the number of realizations is, the more objective the results will be. The effect of the number of realizations on the time-based results has been studied before the production runs conducted in this study. This sensitivity analysis is to determine the minimum number of realizations that are needed to achieve a sufficient degree of objectivity with the results. For this purpose, 100, 500, 1000, and 2000 realizations are considered. Each of these cases is repeated 20 times to obtain the mean values and standard deviations of the respective loss estimates. The variability of the annualized probability of collapse, annualized cost, and annualized fatalities among these repetitions is examined in terms of the mean values and standard deviations of the respective results.

The change of the mean values and standard deviations with the number of realizations for the annualized probability of collapse, annualized cost, and annualized fatalities is shown in Figure 1-39 through Figure 1-41. While the mean values remain practically the same for all the cases, the standard deviations are reduced as the number of realizations increases. Table 1-7 compares the mean values, coefficients of variation (COV) and the computational costs in terms of the time required to run an analysis and the physical memory demand. Based on these data, the number of realizations recommended for such analysis is between 500 and 1000. It has been decided to use 1000 realizations for the analyses conducted in this study because of the reasonable computational cost. Increasing the number of realizations beyond this point increases the computational cost significantly but reduces the scatter by a small amount only.

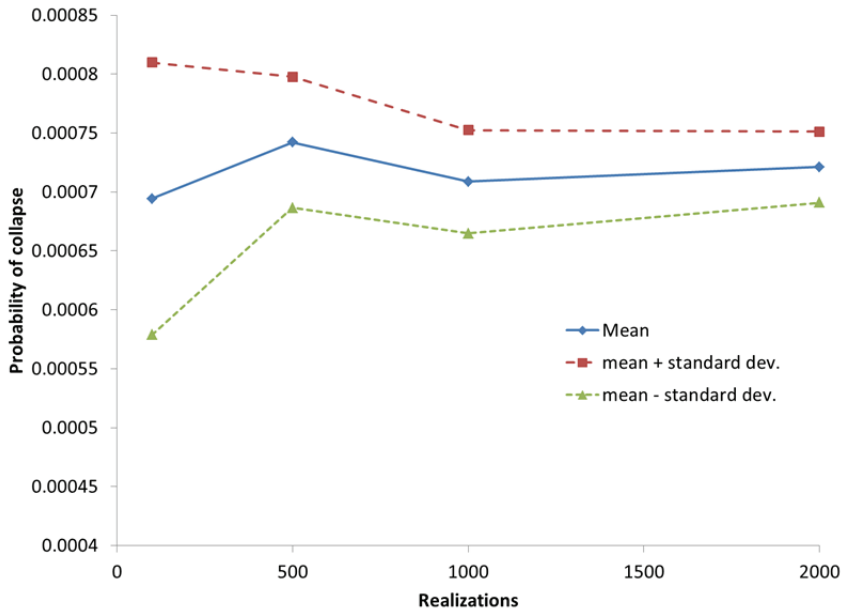

Figure 1-39 Mean and standard deviation of the annualized probability of collapse vs. number of realizations

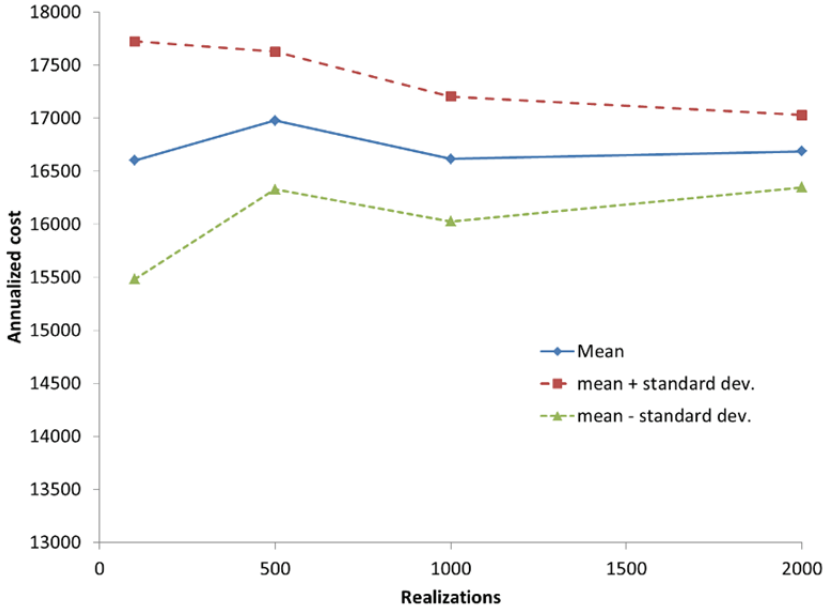

Figure 1-40 Mean and standard deviation of the annualized repair cost vs. number of realizations

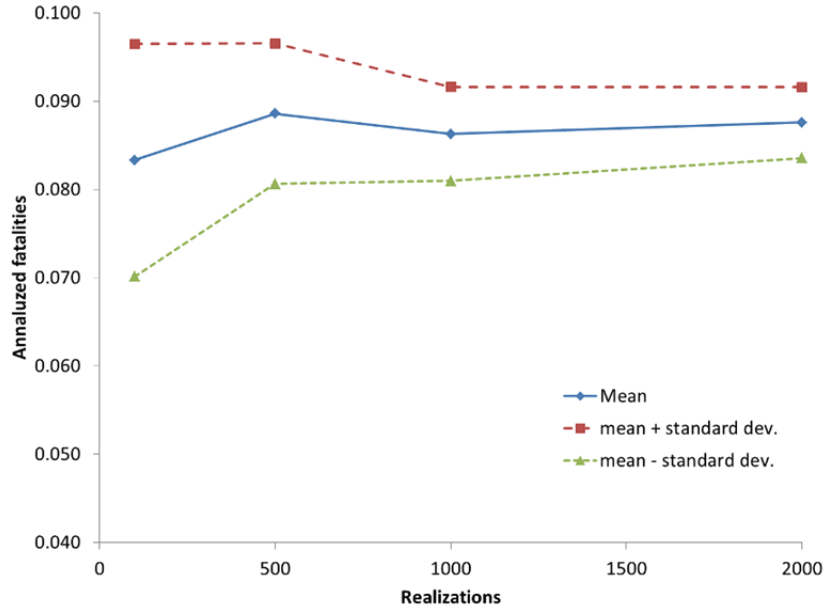

Figure 1-41 Mean and standard deviation of the annualized number of fatalities vs. number of realizations

Table 1-7 Mean, COV and computational cost

	100 realizations		500 realizations		1000 realizations		2000 realizations	
	Mean	COV	Mean	COV	Mean	COV	Mean	COV
Probability of collapse	0.00069	16.6%	0.00074	7.5%	0.00071	6.2%	0.00072	4.2%
Annualized cost ($)	16,601	6.8%	16,976	3.8%	16,615	3.5%	16,688	2.0%
Annualized atalities	0.083	15.8%	0.089	9.0%	0.086	6.2%	0.088	4.6%
Run and saving time (sec) *	5		20		40		70	
Results loading time (sec) *	7		30		60		120	
RAM required (MB)	250		1200		2400		5000	

* Intel Core i7-2600 CPU @ 3.40 GHz (1 processor used only)

Number of intensity stripes in hazard curve

The number of intensity stripes selected to discretize the hazard curve affects time-based assessment results. The larger the number of stripes is, the more accurate the results will be. To illustrate this point, the number of stripes has been modified in the following way.

a) The number of stripes has been reduced from 8 to 4. For this purpose, two consecutive intensity levels (namely, intensity levels 1 and 2, 3 and 4, 5 and 6, and 7 and 8) have been grouped in a single stripe. The demand data from intensities 1+2, 3+4, 5+6, and 7+8 have been averaged to create the demand vectors for the four new stripes. The hazard curve has been also modified and is defined by the midpoints of the new intensity intervals as shown in Table 1-8.

b) The number of stripes has been reduced from 8 to 3. The stripes have been grouped as follows: stripes 1-2 (using the midpoint in 1 as the intensity), stripes 3-5 (using the midpoint in 4 as the intensity), stripes 6-8 (using the midpoint in 7 as the intensity). The new hazard curve is shown in Table 1-8.

Table 1-8 Alternative intensity stripes

No. of Stripes	Intensity Level	S_a(g)	Mean Annual Frequency of Exceedance
4 stripes	1-2	0.328	0.016
	3-4	0.884	0.0024
	5-6	1.44	0.00075
	7-8	2.00	0.0003
3 stripes	1-2	0.189	0.0359
	3-5	1.023	0.00177
	6-8	1.857	0.000381

The time-based results obtained using intensity 4 and 3 stripes are compared with the base case (with 8 strips) in Table 1-9. The use of only 4 stripes leads to an increase of the loss indicators by 20 to 40%, except for the red tagging probability which remains practically the same. Using the coarser hazard curve increases the annualized probability of collapse by 35%. If 3 stripes are used, almost all the main loss indicators are tripled.

In summary, using a coarser discretization of the hazard curve leads to a significant increase in the probability of collapse of the building. The rest of the loss indicators are increased in a similar proportion as the probability of collapse because losses in this building are predominantly caused by collapse.

Table 1-9 Effect of the number of intensity stripes in the time-based assessment results

No. of Stripes	Variable	Value	Change
8 stripes (base case)	Probability of collapse	0.00071	-
	Probability of red tagging	0.0089	-
	Annualized cost ($)	16,615	-
	Downtime (days)	0.685	-
	Annualized fatalities	0.086	-
	Annualized injuries	0.016	-
4 stripes	Probability of collapse	0.00096	35%
	Probability of red tagging	0.0082	-8%
	Annualized cost ($)	20,937	26%
	Downtime (days)	0.863	26%
	Annualized fatalities	0.121	40%
	Annualized injuries	0.019	19%
3 stripes	Probability of collapse	0.00238	236%
	Probability of red tagging	0.0172	92%
	Annualized cost ($)	56,081	238%
	Downtime (days)	2.319	239%
	Annualized fatalities	0.294	240%
	Annualized injuries	0.046	180%

Furthermore, for the base case of 8 stripes, the relative contributions of the higher-intensity stripes to the total loss estimates have assessed by eliminating the higher-intensity stripes in the analysis. Two cases have been studied:

a) The first four lowest stripes (1-4) have been retained, and

b) The first six lowest stripes (1-6) have been retained.

The results presented in Table 1- indicate that the lowest four intensity levels are responsible for 60 to 75% of the total annualized cost, downtime, and human losses; 50% of the collapse; and 85% of the red tagging. They also indicate that the upper two intensity levels contribute to less than 10% of the total annualized cost, downtime, and human losses; 15% of the collapse; and less than 5% of the red tagging. This sensitivity analysis confirms that the low and moderate intensity levels have a significant contribution to the annualized losses. This is the result of the combination of a relatively high probability of occurrence of low intensity motions with the high dispersion of the collapse fragility.

Table 1-10 Effect of removing higher-intensity stripes in the time-based assessment results

Variable	8 Stripes (base case)	Stripes 1-4	Stripes 1-6
Annualized probability of collapse	0.00071	0.00034	0.00061
Annualized probability of red tagging	0.0089	0.0076	0.0086
Annualized total cost ($)	16,615	11,123	15,252
Annualized total downtime (days)	0.685	0.457	0.628
Annualized total no. of fatalities	0.086	0.053	0.078
Annualized total no. of injuries	0.016	0.012	0.015

Contributions of specific fragilities to total loss

To weight the contributions of different fragility groups to the total loss estimates for the building, analyses have been rerun without specific fragility groups, and the results have been compared. For this purpose, the fragilities have been grouped in 5 groups depending on the component types: (a) structural elements (gravity frames and RMSW's); (b) exterior finishes (envelope walls, windows, and roof); (c) interior finishes (partition walls, ceiling, and stairs); (d) services (piping, HVAC, sprinklers, and elevator); and (e) equipment (TV). Only one group is removed at a time. In addition, two analyses have been done without any fragility group to study the contributions of collapse and residual drift to the total loss. In one of these analyses, both collapse and residual drift are considered, and in the other, only collapse is considered.

Time-based results for the different cases are presented in Table 1-10. The probability of collapse for each case is included in this comparison. Although the same collapse fragility is used, there is a very small variation in the probability of collapse entirely due to the random number generation. It should be borne in mind that this small variation could slightly affect other loss estimates.

The main conclusion that can be extracted from this sensitivity study is that the annualized losses expected for this building are to a large extent related to collapse. Based on the values presented in Table 1-10, the annualized repair costs and downtime have the following breakdown: 60% due to collapse, 15% due to demolition for excessive residual drift, 15% due to damage in interior finishes, 5% due to damage in services, and 5% due to damage in structural elements. Almost 100% of the deaths is caused by collapse. The number of deaths resulting from the fall of equipment is very small. The annualized number of injuries has the following breakdown: 55% from

collapse, 30% from damage in interior finishes, and 15% due to damage in equipment and services.

For the annual probability of red tagging, the non-structural components have a major influence, especially those related to services. This is because some of these components, such as fire sprinklers, can easily trigger the red tagging of the building at low intensity levels that have a high probability of occurrence, as shown in Figure 1-37 for intensity 3. The probability of red tagging has the following breakdown: 70% due to damage in services, 15% due to damage in exterior finishes, 10% due to collapse, and 5% due to damage in the remaining fragility groups.

Table 1-10 Effects on loss when removing specific fragility groups

Fragility Groups Included	Variable	Value	Change
All fragility groups included (base case)	Probability of collapse	0.00071	-
	Probability of red tagging	0.0089	-
	Annualized cost ($)	16,615	-
	Downtime (days)	0.68	-
	Annualized fatalities	0.09	-
	Annualized injuries	0.02	-
Structural components removed	Probability of collapse	0.00071	0%
	Probability of red tagging	0.0089	0%
	Annualized cost ($)	15,930	-4%
	Downtime (days)	0.65	-4%
	Annualized fatalities	0.09	2%
	Annualized injuries	0.02	-1%
Exterior finishes removed	Probability of collapse	0.00075	6%
	Probability of red tagging	0.0080	-11%
	Annualized cost ($)	16,347	-2%
	Downtime (days)	0.68	0%
	Annualized fatalities	0.09	5%
	Annualized injuries	0.02	1%
Interior finishes removed	Probability of collapse	0.00075	6%
	Probability of red tagging	0.0087	-2%
	Annualized cost ($)	14,507	-13%
	Downtime (days)	0.58	-15%
	Annualized fatalities	0.09	6%
	Annualized injuries	0.01	-33%
Services removed	Probability of collapse	0.00069	-3%
	Probability of red tagging	0.0045	-50%
	Annualized cost ($)	15,776	-5%
	Downtime (days)	0.66	-4%
	Annualized fatalities	0.08	-3%
	Annualized injuries	0.02	-5%
Equipment removed	Probability of collapse	0.00074	4%
	Probability of red tagging	0.0087	-2%
	Annualized cost ($)	16,734	1%
	Downtime (days)	0.69	1%
	Annualized fatalities	0.08	-2%
	Annualized injuries	0.02	-7%
All fragilities removed	Probability of collapse	0.00068	-4%
	Probability of red tagging	0.0009	-90%
	Annualized cost ($)	11,013	-34%
	Downtime (days)	0.46	-33%
	Annualized fatalities	0.08	-10%
	Annualized injuries	0.01	-48%
All fragilities and residual drift removed	Probability of collapse	0.00072	1%
	Probability of red tagging	0.0007	-92%
	Annualized cost ($)	8,951	-46%
	Downtime (days)	0.36	-48%
	Annualized fatalities	0.08	-6%
	Annualized injuries	0.01	-45%

Number of ground motions

The effect of the number of ground motions used in the nonlinear time-history analysis (i.e., the number of demand vectors) has been studied. For this purpose, the number of ground motion pairs has been increased to 20, and decreased to 7, 5, and 3, as compared to 11 that has been used for the base case. These ground motions have been extracted from a set of 20 ground motion pairs that have been ranked according to how well they match the target spectrum. When using less than 20, the ones that better match the spectral curve are kept. When reducing the number of ground motion pairs to 3, it was not possible to carry out the analysis. This is because, for some intensity levels, once the vectors corresponding to collapse realizations had been removed, only one vector remained. When this happened, the PACT analysis could not be run probably because the covariant matrix could not be computed.

The time-based analysis results with 20, 11, 7 and 5 demand vectors are shown in Table 1-11. When increasing or reducing the number of vectors, the results do not vary much. The cost, downtime, and casualties vary by less than 10%. The differences are small and can be partly attributed to the small variations in the collapse and repair cost probabilities that are affected by the random number generation. Hence, we can conclude that varying the number of ground motions does not affect the results much for this building. However, reducing the number of demand vectors could create a problem when the number becomes very small.

Table 1-11 Effect of the number of ground motions

No. of Ground Motions	Variable	Value	Change
11 (base case)	Annualized probability of collapse	0.00071	-
	Annualized probability of red tagging	0.0089	-
	Annualized total cost ($)	16,615	-
	Annualized total downtime (days)	0.685	-
	Annualized total no. of fatalities	0.086	-
	Annualized total no. of injuries	0.016	-
20	Annualized probability of collapse	0.00067	-6%
	Annualized probability of red tagging	0.0087	-3%
	Annualized total cost ($)	16,154	-3%
	Annualized total downtime (days)	0.667	-3%
	Annualized total no. of fatalities	0.081	-6%
	Annualized total no. of injuries	0.016	-3%
7	Annualized probability of collapse	0.00068	-3%
	Annualized probability of red tagging	0.0078	-12%
	Annualized total cost ($)	16,339	-2%
	Annualized total downtime (days)	0.681	-1%
	Annualized total no. of fatalities	0.083	-4%
	Annualized total no. of injuries	0.015	-9%
5	Annualized probability of collapse	0.00068	-4%
	Annualized probability of red tagging	0.0079	-12%
	Annualized total cost ($)	17,146	3%
	Annualized total downtime (days)	0.710	4%
	Annualized total no. of fatalities	0.083	-3%
	Annualized total no. of injuries	0.015	-10%

Performance groups with correlated and uncorrelated damage

The influence of using performance groups with correlated or uncorrelated damage has been studied. Although it could sometimes be more realistic to assume that damage in a performance group is uncorrelated, the base case assumes that damage is correlated in each performance group to reduce the computational and memory demands for the analysis. The implication of this assumption is studied by comparing the mean values and COV of the time-based results obtained for the base case with the values obtained for the case in which damage is assumed to be uncorrelated. Twenty runs are conducted

for each case. The results are shown in Table 1-12. The computational and memory demands for each of the runs are also included.

Table 1-12 Difference in using performance groups with correlated and uncorrelated damage in time-based results

	Correlated (base case)		Uncorrelated	
	Mean	COV	Mean	COV
Annualized probability of collapse	0.00071	6.2%	0.00070	6.0%
Annualized probability of red tagging	0.0089	2.7%	0.0053	3.3%
Annualized total cost ($)	16,615	3.5%	16,814	3.7%
Annualized total downtime (days)	0.685	3.6%	0.660	3.2%
Annualized total no. of fatalities	0.086	6.2%	0.093	4.7%
Annualized total no. of injuries	0.016	5.5%	0.017	3.1%
Run and saving Time (sec)	40		210	
Results loading Time (sec)	60		320	
RAM required (MB)	2400		12000	

The mean values of the loss indicators, except red tagging, are very similar for both cases. Their difference is 7% or less. In addition, the coefficients of variations are of the same order of magnitude. The only result that changes in a significant way is the probability of red tagging. When damage is uncorrelated, the probability of red tagging drops by 40%. Intensity-based results obtained in a single run are compared in Table 1-13, and they also show that the only significant difference between the correlated and uncorrelated cases is the probability of red tagging.

Figure 1-42 shows the probability of red tagging for intensity 3. When compared to Figure 1-37, one can observe that the red tagging probability related to all component fragility groups is reduced when damage is uncorrelated. In particular, the probability of red tagging due to the damage of fire sprinklers (D4011.013a) is reduced from 35 to 20%. This difference is due to the fact that the building is red tagged when a specified fraction of a performance group has reached a specific damage level. For a performance group with correlated damage, damage is either 0 or 100%. As a result, the probability of this group triggering a red tag is identical to the probability of having any one of its components reach the red-tag level. For a performance group with uncorrelated damage, some components could be damaged to the red tag level, but the total number may not reach the fraction that warrants red tagging.

Table 1-13 Effects of using performance groups with correlated and uncorrelated damage in intensity-based results

Int.	Variable	Correlated (base case)			Uncorrelated		
		Mean	10th Percentile	90th Percentile	Mean	10th Percentile	90th Percentile
1	Repair Cost ($)	4,358	*	12,333	4,717	*	12,785.71
	Downtime (days)	0.31	*	0.75	0.33	*	0.79
	No. of Fatalities	0.00	*	*	0.00	*	0.002
	No. of Injuries	0.00	*	*	0.00	*	0.006
2	Repair Cost ($)	194,969	13,876	259,375	204,612	15,408	233,333
	Downtime (days)	10.71	1.04	14.29	10.94	1.11	9.99
	No. of Fatalities	0.61	*	0.78	0.86	0.03	0.90
	No. of Injuries	0.33	*	0.38	0.32	0.00	0.66
3	Repair Cost ($)	902,941	84,746	915,789	856,677	109,871	805,263
	Downtime (days)	45.13	2.24	40.45	43.18	2.15	31.84
	No. of Fatalities	4.93	*	0.90	4.59	0.09	0.94
	No. of Injuries	0.96	*	1.88	0.96	0.02	1.87
4	Repair Cost ($)	2,646,843	329,545	11,939,394	2,518,243	338,542	11,935,484
	Downtime (days)	125.31	11.31	493.90	119.92	11.56	493.55
	No. of Fatalities	13.41	*	63.49	12.14	0.11	43.00
	No. of Injuries	2.20	*	8.45	2.07	0.03	7.07
5	Repair Cost ($)	4,583,670	525,882	11,967,742	4,901,864	580,000	11,970,326
	Downtime (days)	210.02	17.60	496.77	223.46	20.80	497.03
	No. of Fatalities	22.47	0.01	99.50	23.55	0.13	115.00
	No. of Injuries	3.31	0.02	11.70	3.52	0.07	12.80
6	Repair Cost ($)	5,741,077	700,000	11,975,309	6,071,639	765,000	11,977,117
	Downtime (days)	259.43	26.13	497.53	271.74	27.29	497.71
	No. of Fatalities	31.58	0.07	123.33	36.12	0.15	139.00
	No. of Injuries	4.61	0.06	14.50	4.84	0.13	15.40
7	Repair Cost ($)	6,837,841	747,727	11,980,431	6,752,408	857,895	11,980,080
	Downtime (days)	301.04	27.82	498.04	297.73	31.07	498.01
	No. of Fatalities	47.04	0.11	152.16	45.56	0.17	150
	No. of Injuries	6.00	0.07	16.93	5.93	0.16	16.74
8	Repair Cost ($)	8,337,682	1,188,889	11,984,127	8,591,736	1,429,412	11,984,756
	Downtime (days)	365.36	45.35	498.41	374.29	55.38	498.48
	No. of Fatalities	56.82	0.16	163.33	56.97	0.21413	157.00
	No. of Injuries	7.18	0.11	18.23	7.27	0.36	17.40

* The probability of no loss is higher than the percentile indicated.

The CPU time required to run and save the results and the physical memory needed for an analysis with all performance groups having uncorrelated damage is about 5 times those for a correlated case. Hence, it seems that the small change in loss estimates (other than red tagging) does not justify the use of performance groups with uncorrelated damage, which has much higher computational demands.

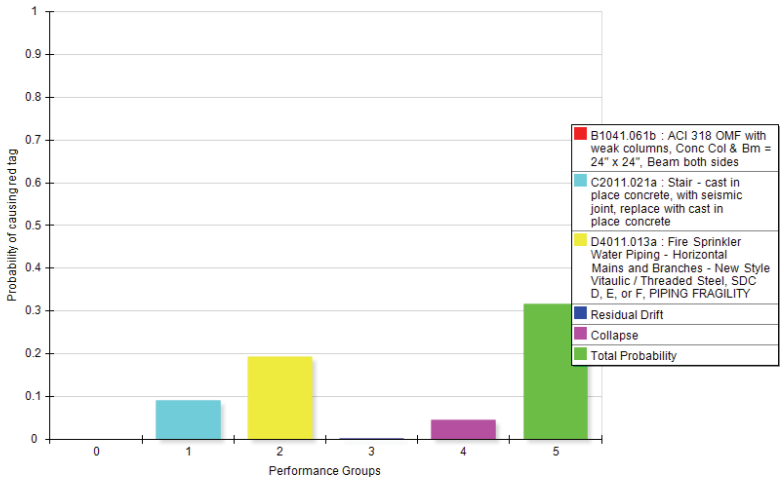

Figure 1-42 Probability of red tagging for performance groups with uncorrelated damage for intensity 3

Residual drift demand and reparability fragility

The influence of the variation in the residual drift demand and reparability fragility on time-based loss results has been studied. From the demand standpoint, the base case uses the method proposed by ATC-58 to calculate the residual story drift based on the peak story drift obtained from nonlinear time-history analysis. As an alternative, the residual story drifts obtained directly from analysis can be used. The magnitude of the residual drifts obtained directly from analysis is significantly smaller. This can be explained by the rocking behavior of the wall and by the fact that possible base sliding is neglected in the analysis. Results of the loss assessment for these two cases are presented in Table 1-14. When using the results directly from structural analysis, the cost and downtime are reduced by 14%. In fact, this reduction is practically the same as the contribution of the residual drift to the loss indicators for the base case, as presented in a previous section. This means that when using the actual analysis results, the effect of the residual drift on the total losses is insignificant.

Table 1-14 Influence of methods to calculate residual drift demand on time-based analysis results

Method	Variable	Value	Change
ATC-58 method (base case)	Annualized probability of collapse	0.00071	-
	Annualized probability of red tagging	0.0089	-
	Annualized total cost ($)	16,615	-
	Annualized total downtime (days)	0.685	-
	Annualized total no. of fatalities	0.086	-
	Annualized total no. of injuries	0.016	-
Directly from structural analysis	Annualized probability of collapse	0.00067	-1%
	Annualized probability of red tagging	0.0087	-1%
	Annualized total cost ($)	16,154	-14%
	Annualized total downtime (days)	0.667	-14%
	Annualized total no. of fatalities	0.081	-1%
	Annualized total no. of injuries	0.016	0%

To investigate the influence of the properties of the reparability fragility function which has residual drift as the demand parameter, the median of the distribution has been varied from 1%, for the base case, to 2 and 0.5%, respectively. A case without the reparability consideration, which is equivalent to assuming an infinite median for the fragility curve, has also been run. The results are presented in Table 1-15. When the median residual drift is reduced to 0.5%, the cost and downtime increase by 40%. The small variations of the other loss indicators are due to the random number generation. When increasing the median to 2%, the reduction in cost and downtime is 12%. When the median drift is increased to infinity, the reduction is 15%. The magnitude of this reduction is consistent with the results presented earlier.

Table 1-15 Influence of the median of reparability fragility on time-based analysis results

Median of Fragility	Variable	Value	Change
1% (base case)	Annualized probability of collapse	0.00071	-
	Annualized probability of red tagging	0.0089	-
	Annualized total cost ($)	16,615	-
	Annualized total downtime (days)	0.685	-
	Annualized total no. of fatalities	0.086	-
	Annualized total no. of injuries	0.016	-
0.5%	Annualized probability of collapse	0.00075	6%
	Annualized probability of red tagging	0.0090	1%
	Annualized total cost ($)	22,988	38%
	Annualized total downtime (days)	0.955	40%
	Annualized total no. of fatalities	0.090	4%
	Annualized total no. of injuries	0.017	1%
2%	Annualized probability of collapse	0.00070	-1%
	Annualized probability of red tagging	0.0089	0%
	Annualized total cost ($)	14,625	-12%
	Annualized total downtime (days)	0.602	-12%
	Annualized total no. of fatalities	0.085	-1%
	Annualized total no. of injuries	0.016	-3%
Infinite	Annualized probability of collapse	0.00071	0%
	Annualized probability of red tagging	0.0088	-2%
	Annualized total cost ($)	14,258	-14%
	Annualized total downtime (days)	0.585	-15%
	Annualized total no. of fatalities	0.085	-2%
	Annualized total no. of injuries	0.016	-4%

Collapse fragility and mode

The sensitivity of the loss results to the collapse fragility and mode assumed has been studied. The differences in the results when the median of the collapse fragility is doubled and halved with respect to the base case are presented in Table 1-16. The effect of assuming no collapse, i.e. an infinite median, is also presented. When halving the median, the annualized probability of collapse is increased by 5.5 times, the fatalities by 4 times, and the cost, downtime, and injuries by 2 times. The increase in the probability of red tagging is only 17%. When doubling the median, the annualized

probability of collapse and number fatalities is 10 times smaller, the cost, downtime, and injuries are 2 times smaller, and the red tagging does not vary. When no collapse is considered, the cost, downtime, and injuries are cut almost by half, and the number of deaths is reduced by 100 times. This confirms the strong influence of collapse in the total loss. It also shows that the non-structural component fragilities can cause a significant number of injuries but a very small number of deaths.

Table 1-16 Influence of collapse fragility on time-based analysis results

Median Spectral Intensity	Variable	Value	Change
2.1g (base case)	Annualized probability of collapse	0.00071	-
	Annualized probability of red tagging	0.0089	-
	Annualized total cost ($)	16,615	-
	Annualized total downtime (days)	0.685	-
	Annualized total no. of fatalities	0.086	-
	Annualized total no. of injuries	0.016	-
1.05g	Annualized probability of collapse	0.00394	455%
	Annualized probability of red tagging	0.0105	17%
	Annualized total cost ($)	53,045	219%
	Annualized total downtime (days)	2.214	223%
	Annualized total no. of fatalities	0.440	409%
	Annualized total no. of injuries	0.054	230%
4.2g	Annualized probability of collapse	0.00007	-89%
	Annualized probability of red tagging	0.0089	-1%
	Annualized total cost ($)	9,847	-41%
	Annualized total downtime (days)	0.400	-42%
	Annualized total no. of fatalities	0.015	-83%
	Annualized total no. of injuries	0.009	-45%
Infinite	Annualized probability of collapse	0	-100%
	Annualized probability of red tagging	0.0088	-1%
	Annualized total cost ($)	9,340	-44%
	Annualized total downtime (days)	0.383	-44%
	Annualized total no. of fatalities	0.0006	-99%
	Annualized total no. of injuries	0.0084	-49%

The collapse mode has been changed from a total collapse mode to a partial collapse mode where the debris coverage ratio is 0.9 of the first floor and 0.1 of the second. The same rates of deaths and injuries are kept. Results for this

two collapse modes are presented in Table 1-17. When a partial collapse is considered, the number of deaths is cut by half, and the number of injuries by one fourth. The rest of the loss indicators do not vary. The probability of collapse and the repair cost have to remain the same because the collapse fragility and the replacement cost do not change.

Table 1-17 Influence of collapse mode on time-based analysis results

Collapse Mode	Variable	Value	Change
Total collapse (base case)	Annualized probability of collapse	0.00071	-
	Annualized probability of red tagging	0.0089	-
	Annualized total cost ($)	16,615	-
	Annualized total downtime (days)	0.685	-
	Annualized total no. of fatalities	0.086	-
	Annualized total no. of injuries	0.016	-
Partial collapse	Annualized probability of collapse	0.00072	2%
	Annualized probability of red tagging	0.0090	1%
	Annualized total cost ($)	16633	0%
	Annualized total downtime (days)	0.687	0%
	Annualized total no. of fatalities	0.047	-45%
	Annualized total no. of injuries	0.012	-27%

Modeling dispersion

The sensitivity of the loss results to the value assumed for the modeling dispersion has been studied. The effects of increasing this dispersion from 0.35 (base case) to 0.5 and of decreasing it to 0.14 on time-based results are presented in Table 1-18. This range represents the limits of the values recommended in Volume 1 of the 90% draft of the ATC-58 Guidelines. The differences for all the loss indicators are smaller than 5% and they can be attributed to the random number generation. Hence, the effect of varying the modeling dispersion within this range on the results is not significant. The mean, and the 10th and 90th percentile values from intensity-based analyses using the different modeling dispersion values are shown in Table 1-19. These results are also very similar to those obtained for the base case, which are shown in Table 1-2.

Table 1-18 Influence of modeling dispersion on time-based analysis results

Modeling Dispersion	Variable	Value	Change
0.35 (base case)	Annualized probability of collapse	0.00071	-
	Annualized probability of red tagging	0.0089	-
	Annualized total cost ($)	16,615	-
	Annualized total downtime (days)	0.685	-
	Annualized total no. of fatalities	0.086	-
	Annualized total no. of injuries	0.016	-
0.14	Annualized probability of collapse	0.00075	5%
	Annualized probability of red tagging	0.0088	-2%
	Annualized total cost ($)	16,855	1%
	Annualized total downtime (days)	0.697	2%
	Annualized total no. of fatalities	0.090	5%
	Annualized total no. of injuries	0.017	1%
0.5	Annualized probability of collapse	0.00069	-2%
	Annualized probability of red tagging	0.0092	3%
	Annualized total cost ($)	16,630	0%
	Annualized total downtime (days)	0.689	1%
	Annualized total no. of fatalities	0.084	-3%
	Annualized total no. of injuries	0.017	2%

Table 1-19 Influence of modeling dispersion on intensity-based analysis results

Int.	Variable	Model Dispersion: 0.14			Model Dispersion: 0.5		
		Mean	10th Percentile	90th Percentile	Mean	10th Percentile	90th Percentile
1	Repair Cost ($)	1,583	- *	2,657.14	9,793	- *	24,062.50
	Downtime (days)	0.11	- *	0.16	0.69	- *	1.57
	No. of Fatalities	0.00	- *	- *	0.00	- *	- *
	No. of Injuries	0.00	- *	- *	0.02	- *	- *
2	Repair Cost ($)	161,203	13,684	277,419	175,496	11,799	238,182
	Downtime (days)	9.30	1.02	14.30	9.62	0.92	11.85
	No. of Fatalities	0.59	- *	0.79	0.93	- *	0.78
	No. of Injuries	0.32	- *	0.38	0.34	- *	0.28
3	Repair Cost ($)	1,018,916	86,207	910,000	870,625	98,039	847,368
	Downtime (days)	50.28	2.35	44.07	44.02	2.33	40.43
	No. of Fatalities	5.46	- *	0.91	4.26	- *	0.90
	No. of Injuries	1.06	- *	2.37	0.93	- *	1.80
4	Repair Cost ($)	2,588,716	309,574	11,938,272	2,738,803	328,261	11,941,860
	Downtime (days)	122.51	11.21	493.83	130.02	11.50	494.19
	No. of Fatalities	13.20	- *	62.00	13.90	- *	68.33
	No. of Injuries	2.24	- *	8.70	2.29	- *	8.73
5	Repair Cost ($)	4,506,077	517,308	11,967,105	4,803,248	552,000	11,969,789
	Downtime (days)	207.58	18.60	496.71	219.26	19.89	496.98
	No. of Fatalities	22.22	- *	106.00	23.62	- *	113.50
	No. of Injuries	3.51	0.02	12.85	3.63	- *	13.37
6	Repair Cost ($)	6,171,931	718,868	11,977,578	5,764,558	658,140	11,975,430
	Downtime (days)	275.83	26.49	497.76	260.41	23.64	497.54
	No. of Fatalities	35.56	0.05	136.67	34.46	0.06	143.00
	No. of Injuries	4.85	0.06	15.35	4.77	0.05	16.10
7	Repair Cost ($)	6,584,822	745,652	11,979,424	7,099,279	763,830	11,981,378
	Downtime (days)	291.76	27.23	497.94	311.40	28.65	498.14
	No. of Fatalities	45.63	0.09	148	52.05	0.10	159
	No. of Injuries	5.93	0.07	16.83	6.61	0.07	17.67
8	Repair Cost ($)	8,191,762	1,147,619	11,983,845	8,253,782	1,173,333	11,984,000
	Downtime (days)	358.03	43.45	498.38	360.78	46.67	498.40
	No. of Fatalities	55.14	0.155507	154.50	55.79	0.172995	155.80
	No. of Injuries	7.22	0.11	17.40	7.28	0.13	17.48

* The probability of no loss is higher than the percentile indicated.

Population

The type of building population has been modified from a hotel to an elementary school to study the effect of the occupancy model on the results. Using the default values for an elementary school, the peak occupancy increases to 14 occupants per 1,000 sq. ft. and the variation with time also changes, as shown in Figure 1-43 with the original population model presented in Figure 1-8.

By changing the population model, the only results that change noticeably are those related to the number of casualties. As shown in Table 1-20, the number deaths and injuries increase by 37% and 31%, respectively. This increase is not as large as the increase in the peak occupancy density (350%) because the average occupancy density is not so different. The rest of the loss estimates remain unchanged as expected, and their difference is only due to the random number generation.

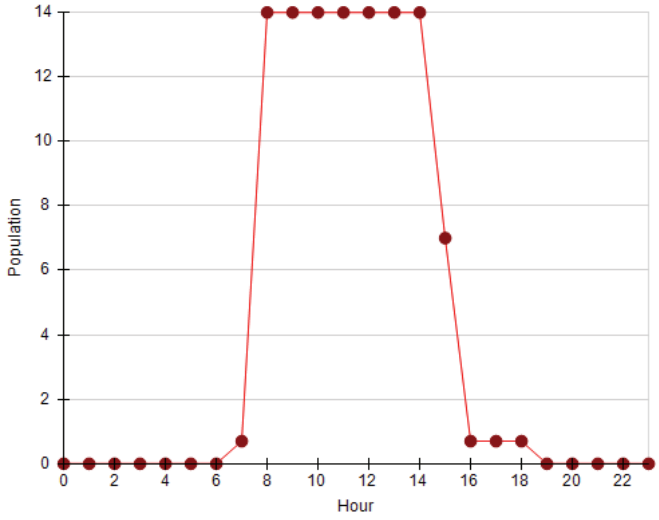

Figure 1-43 Population model for a school building on a regular school day

User-defined anchorage fragility

The influence of the anchorage fragilities on the loss results has been studied by modifying the median of their distribution functions. In particular, the median for the user-defined anchorage fragilities, namely those corresponding to electrical components (D5011.013g, D5012.023d, D5012.033d), has been halved and doubled with respect to the base case. The results presented in Table 1-21 show that these changes do not have a noticeable influence on the loss results.

Table 1-20 Influence of population model on time-based analysis results

Population	Variable	Value	Change
Hotel (base case)	Annualized probability of collapse	0.00071	-
	Annualized probability of red tagging	0.0089	-
	Annualized total cost ($)	16,615	-
	Annualized total downtime (days)	0.685	-
	Annualized total no. of fatalities	0.086	-
	Annualized total no. of injuries	0.016	-
School	Annualized probability of collapse	0.00071	1%
	Annualized probability of red tagging	0.0089	-1%
	Annualized total cost ($)	16,892	2%
	Annualized total downtime (days)	0.696	2%
	Annualized total no. of fatalities	0.119	37%
	Annualized total no. of injuries	0.022	31%

Table 1-21 Influence of user-defined anchorage fragility on time-based analysis results

Median Spectral Intensity	Variable	Value	Change
2g (base case)	Annualized probability of collapse	0.00071	-
	Annualized probability of red tagging	0.0089	-
	Annualized total cost ($)	16,615	-
	Annualized total downtime (days)	0.685	-
	Annualized total no. of fatalities	0.086	-
	Annualized total no. of injuries	0.016	-
4g	Annualized probability of collapse	0.00073	2%
	Annualized probability of red tagging	0.0089	0%
	Annualized total cost ($)	16,735	1%
	Annualized total downtime (days)	0.691	1%
	Annualized total no. of fatalities	0.089	3%
	Annualized total no. of injuries	0.017	1%
0.5g	Annualized probability of collapse	0.00073	3%
	Annualized probability of red tagging	0.0089	0%
	Annualized total cost ($)	16,721	1%
	Annualized total downtime (days)	0.688	1%
	Annualized total no. of fatalities	0.088	2%
	Annualized total no. of injuries	0.017	1%

1.1.8 Possible Improvements for the PACT Software

The following comments and recommendations are given for possible improvements to the input of the building data:

- When populating a building, it would be useful to have an option that automatically defines the fragility and performance groups, and the respective quantities for the given building type based on the normative quantities recommended in ATC-58. The user could then add or remove performance groups, and modify the default quantities.
- It would be helpful to compare the replacement cost of the building that is entered in the building information tab with the maximum possible repair cost computed from all the performance groups. Once all fragility and performance groups have been defined, PACT could provide this information.
- In the performance groups tab, it would be very useful to show the units of the quantities (e.g., sq.ft., 100 sq.ft, etc.) that have to be introduced for each group.
- In the nonlinear analysis tab, it is tedious to copy and paste the results for each intensity level, each level of the building, each demand parameter, and each direction. It would be very convenient to be able to import results from a single file in a single step.

The following comments and recommendations are given for possible improvements to the performance evaluation algorithms:

- The speed of the computation has been significantly improved with respect to the previous version. However, it takes more time to open and save the results than to run the analysis. The physical memory needed to run and read the results is still very high. Improvements to reduce the amount of required hard memory would be helpful.

The following comments and recommendations are given for possible improvements to the presentation of the results:

- An option to export the time-based results (annualized probability curves) in tabular form would be helpful.
- For the time-based results, it would be very useful to visualize the contribution of each fragility group or a set of fragilities to the annualized total repair cost, annualized downtime, annualized probability of red tagging, and annualized number of casualties. This evaluation has been done in this study by removing performance groups and observing the difference in the results. An automated process would be useful for

an easy identification of the most critical components and upgrading needs.

For RMSW's, the following statement may be included as a comment in the description of the fragility specification in the fragility manager of PACT: "In a multi-story cantilever wall, much of the story drift in an upper story can be caused by the rigid-body rotation induced by the flexural deformation in the lower stories. This rigid-body rotation should be taken out from the story drift not to over-estimate the flexural demand on the wall component."

1.1.9 Summary of Findings

The main findings from the seismic performance assessment of the two-story reinforced masonry building using PACT 2 Beta are listed below:

- The estimated collapse risk of this building is relatively high due to the high dispersion of the collapse fragility. The high dispersion causes non-negligible probabilities of collapse for low intensities, which results in an elevated probability of collapse for the time-based analysis because of the high probability of low-intensity motions.
- Practically all the fatalities are caused by collapse in this assessment. A small number of deaths, about 1% of the annualized number, are caused by the fall of TV sets.
- Half of the injuries are caused by collapse and half as a consequence of damage in the building components, mainly interior finishes, services and TV sets.
- For this building, 60% of the repair costs and downtime are attributed to collapse. This cannot only be explained by the relatively high dispersion for the probability of collapse of the building, but also by the fact that the building has not been fully populated with component fragility groups. Some fragility groups are not available in PACT (e.g appliances and furniture). As a result, while the replacement cost for the total collapse is set at $12M, the maximum repair cost estimated from a non-collapse realization is $7M.
- For this building, demolition due to excessive residual drift represents 15% of the annualized cost and downtime. Besides collapse and residual drift, repair costs and downtime are due to damage in interior finishes (partitions) and services (piping) of the building. Excluding collapse, damage in structural elements represents only 5% of the total annualized cost and downtime.

- The probability of red tagging is the only variable that strongly depends on the properties of the component fragility functions. Non-structural components are responsible for most of the red tagging probability.
- For this building, losses are mainly caused by collapse and excessive residual drift. Sensitivity analyses have shown that these results are very sensitive to the collapse and residual drift fragility parameters and to the residual drift demands assumed. It is, therefore, important to provide good estimations for these parameters.
- It is recommended to use nonlinear time-history analysis instead of the simplified analysis. For this building, some demand quantities from the simplified analysis are much lower than those from the nonlinear analysis, and the losses are, therefore, likely to be under-estimated.
- To obtain accurate loss estimation, it is recommended to use a high number of realizations. The number of realizations needed has to be defined on a case-to-case basis to balance accuracy and computational cost.
- Performance groups with correlated or uncorrelated damage do not seem to affect the results noticeably .
- Using a small number of intensity stripes, namely, 4 and 3, leads to significantly different time-based analysis results as compared to using 8 stripes.
- The value assumed for the modeling dispersion does not have a noticeable influence on the final results if it is in the range of values recommended in Volume 1 of the 90% draft of the ATC-58 Guidelines.
- It is not required to use a very large number of ground motions (demand vectors) in nonlinear time-history analysis. However, this number has to be sufficiently high to avoid ending up with a very small number of demand vectors once the realizations resulting in collapse have been removed. At least two vectors per intensity level have to be provided to be able to run PACT.

1.1.10 Appendix: PACT (Beta Version) Error Reports

Error 1. Residual drift demand vector

The residual drift demands for the lower intensities are zero for all the ground motions. However, when these demands are introduced in PACT, the analysis does not run, probably because it is not possible to establish a probability distribution for the residual drift demands. See error message below.

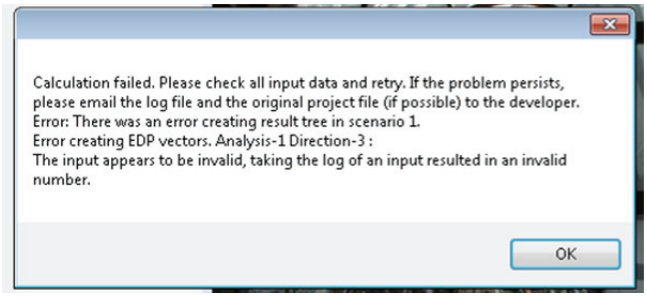

To circumvent this problem, the residual drift demands at the lower levels have been made up using very small values.

Error 2. Hazard curve

Depending on the way the hazard curve is defined, PACT is not able to plot this curve (see first figure below) sometimes, or the plot may have a strange shape (see second figure below) with kinks that indicate that in some regions the probability of occurrence increases with the value of the spectral acceleration. This error should be corrected. However, we do not think that this error has an influence in the loss assessment because only the mid-point in each interval defined in tabular form what is used in the analysis.

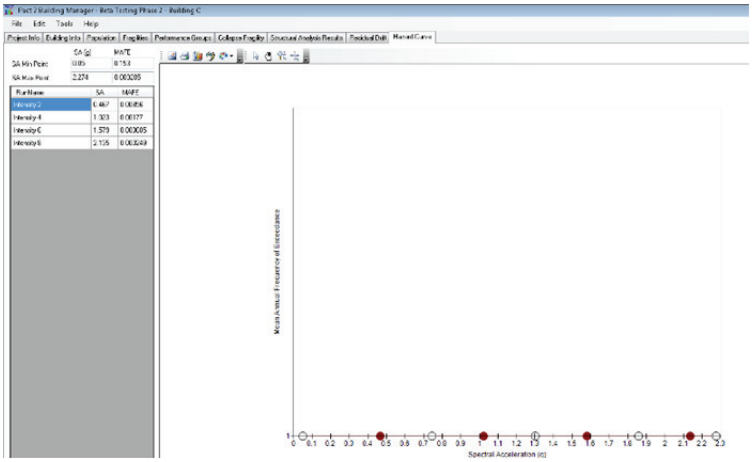

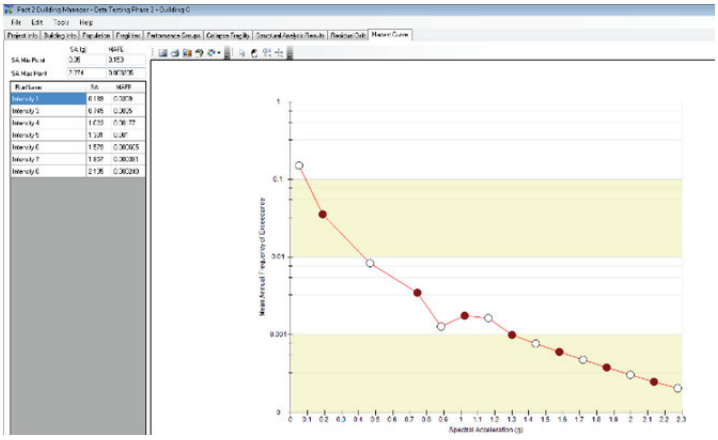

Error 3. Adding a new demand parameter.

A third demand parameter, the modified story-drift ratio, was needed to carry out the fragility analysis of the masonry shear walls. The method presented on page C-14 of Volume 2 of the 90% draft, which is described below, for adding a new demand parameter did not work in our trial.

In addition to the commonly used interstory drift and floor acceleration demand parameters, you can also specify special or custom demand parameters using the PACT Demand Parameter Selection block menu (See Figure 4-20). For example, if you have defined fragility for door frames and doors can jam if residual drift exceeds a certain value, you may define residual drift ratio as a new Special EDP. Once you do that, when your proceed to importation of analysis results, PACT will ask you to provide residual drift ratio values in addition to other demand parameters.

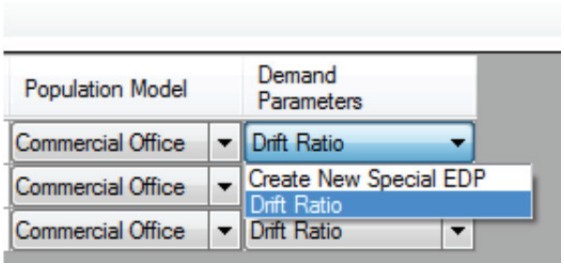

Figure C.5.19 PACT Demand Parameter Selection data block.

When this procedure was followed, the analysis did not run (see the error message below).

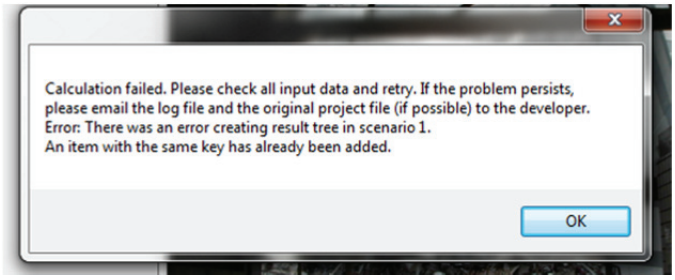

However, the following method was successfully used to add the new demand parameter for the shear walls.

1) Modify the fragility specification in fragility manager to add a new EDP to the fragility group as shown below.

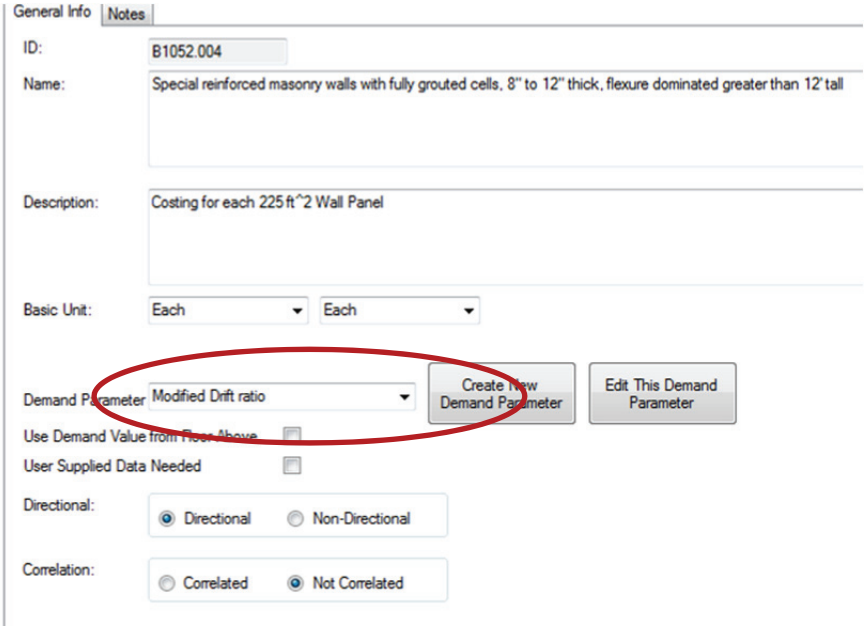

2) Include the modified fragility group in the respective performance groups. Then, the new EDP appears automatically as shown.

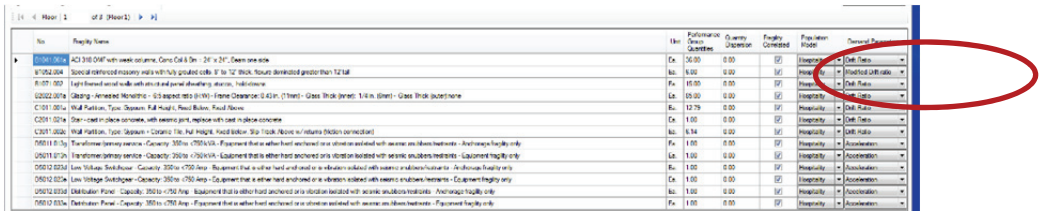

3) Provide analysis results for new EDP.

The analysis was able to run following this approach.

Error 4. Normative sheet

There is an error in the normative value for the quantity of windows in hospitality buildings. The normative value is for the fragility group *B2022.001a Glazing - Annealed Monolithic - 6:5 aspect ratio (H:W) - Frame Clearance: 0.43 in. (11mm) - Glass Thick (inner): 1/4 in. (6mm) - Glass Thick (outer):none*. The normative quantity obtained from PACT is 100 times smaller than what was recommended in a previous version. The previous value seems more reasonable and has been used here. The normative value for this fragility group should be corrected.

In addition, this Excel sheet recommends including piping fragilities but not the corresponding bracing fragilities. We think that these groups should be included too.

1.1.11 References

ASCE/SEI 7-05 (2005), Minimum Design Loads for Buildings and Other Structures, ASCE/SEI.

ATC (2009), Quantification of Building Seismic Performance Factors (FEMA P695), Applied Technology Council, Redwood City, CA.

ATC (2011), ATC-58: Guidelines for Seismic Performance Assessment of Buildings (90% Draft), Applied Technology Council, Redwood City, CA.

Koutromanos, Y. and Shing, P.B. (2010), "Application of the FEMA 695 (ATC-63) Methodology for the Collapse Performance Evaluation of Reinforced Masonry Shear Wall Structures", Proceedings of the 9th U.S. National and 10th Canadian Conference on Earthquake Engineering, Toronto, Canada.

MSJC (2008), Building Code Requirements for Masonry Structures (TMS 402-08 / ACI-530-08 / ASCE 5-08), The Masonry Society, American Concrete Institute, and ASCE/Structural Engineering Institute.

Murcia-Delso, J. and Shing, P.B. (2009), "Damage States and Fragility Curves for Reinforced Masonry Shear Walls." Report No. SSRP–09/14, Department of Structural Engineering, University of California, San Diego, La Jolla, CA.

Shing, P.B., Noland, J.L., Spaeh, H.P., Klamerus, E.W., and Schuller, M.P. (1991), "Response of Single-Story Reinforced Masonry Shear Walls to In-Plane Lateral Loads*", Report No. 3.1(a)-2*, US-Japan Coordinated Program for Masonry Building Research, University of Colorado at Boulder, Boulder, CO.